

## Response to Referee #1

We would like to thank the referee for their insightful comments and have responded below. The referee comments are highlighted in red with our responses in black.

Review of “An instrument for quantifying heterogeneous ice nucleation in multiwell plates using infrared emissions to detect freezing” by Harrison et al. General comments: I support publication of this manuscript in AMT. The research aligns well with the scope of AMT. The reviewer finds the application of release of latent heat for detecting a freezing event in immersion mode ice spectrometer unique. The authors successfully present the applicability of their technique (IR-NIPI) to characterize immersion freezing efficiencies of three different forms of the sample (incl. chips, powder and ambient particles collected on the filter and scrubbed with water) at  $T > -22$  °C. In particular, its applicability to the atmospheric sample seems promising the reviewer finds Figs. 8 and 9 nice and elegant. With further improvements in the temperature uncertainty ( $\pm 0.9$  °C is reported in the manuscript) and applicability in different droplet volumes (so, wider T coverage), IR-NIPI may become very versatile in the INP research (specifically for biological high-T INPs). The review has only minor (but important) comments.

### Comments

P1 L11-13: The main focus of the presented work is on novel application of latent heat in immersion freezing spectrometry, and the reviewer finds the discussion of online vs. offline unnecessary (especially in the abstract). L12-13 is erroneous – some cloud simulation chambers can assess multiple Ts. The reviewer strongly suggests removing “While instruments . . . Hence,”.

Accepted, we agree and have removed this piece of text from the abstract.

P2 L36-38: Reference suggestion - Hande, L. B., and Hoose, C.: Partitioning the primary ice formation modes in large eddy simulations of mixed-phase clouds, *Atmos. Chem. Phys.*, 17, 14105–14118, 2017.

Thank you. We have now added this reference.

P2 L40: ~1 L-1 at what temperature? Please clarify to the readers.

The study was of three case studies of cloud fields. The temperature at which this concentration was reached depended on the local INP spectrum. It is quite challenging to insert this information without distracting from the main point of the statement hence we would rather leave it as is.

P2 L42-43: Plus developing realistic but computationally inexpensive parameterization is also a key to what is addressed here by the authors.

We have changed the text to read “The ability to quantify INP spectra (INP concentrations as a function of temperature) and test the efficiency of proxy materials for ice-nucleating efficiency is invaluable for improving our understanding of cloud glaciation and developing computationally inexpensive parameterisations for atmospheric models.”

P2 L45: Quantitatively define “warmer temperatures” perhaps with specific reference(s). L51-53 implies -11 °C as warmer temperatures?

We have altered the text to read “However it is not a trivial task, in part because INP concentrations are low ( $< 0.1 \text{ L}^{-1}$ ) (DeMott et al., 2010) and the sites on the surfaces which cause nucleation at warm temperatures (Whale et al., 2017; Vali, 2014) are rare.”

P3 L61-63: What about the Arctic? Some discussions may benefit the paper.

We agree that the Arctic is similarly low in INP concentrations, hence expect a similar situation to the southern ocean. We have now discussed this. “This can be improved with aerosol concentrators (Prezzi et al., 2013; Tobo et al., 2013), but is still above the INP concentrations models suggest influence the properties of certain cloud types, such as low/high latitude cold-sector clouds (Vergara-Temprado et al., 2018).”

P3 L71: Reference suggestion - Stopelli, E. et al.: Freezing nucleation apparatus puts new slant on study of biological ice nucleators in precipitation, *Atmos. Meas. Tech.*, 7, 129–134, 2014.

This has been added. In addition we have added Conen et al. 2012.

P3 L71: The reviewer thinks the discussion of previous studies applying latent heat release as an asset for ice nucleation research will benefit the paper. Please consider include and discuss; e.g., Marcolli, C. et al.: Efficiency of immersion mode ice nucleation on surrogates of mineral dust, *Atmos. Chem. Phys.*, 7, 5081-5091, 2007.

We agree a discussion of this paper should be made and have added the following text in a new section where we also discuss other instruments one of the other referees highlighted: “While many instruments use optical cameras to detect freezing events (Whale et al., 2015; Budke and Koop, 2015; Häusler et al., 2018; Beall et al., 2017), , some researchers have used techniques which detect the release of latent heat associated with freezing.. For example, differential scanning calorimetry (Marcolli et al. 2007; Pinti et al. 2012) and infrared emissions (Zaragotas et al., 2016; Kunert *et al.* 2018) have been used.

P4 L99: ns(T)

Done

P5 L140-141: Very important statement – recap this point (sharp rise in  $T = +2\text{ }^{\circ}\text{C}$ ) in the abstract and/or conclusion section.

We have recapped this in the conclusion “A freezing event is detected as a sharp rise in freezing temperature to the equilibrium melting point and a novel calibration method has been proposed which relies on the return of water droplets to the equilibrium melting temperature of water,  $0^{\circ}\text{C}$ , after initial freezing.” The sharp rise in temperature is already referred to in the abstract.

P6 L142-145: The authors may want to rephrase this part and explain the points more intuitively

We have reworded this section so that the reader may better understand the points made. “The  $2^{\circ}\text{C}$  threshold occasionally needs to be optimised to capture freezing events while eliminating the detection of false freezing events. For example, samples that freeze above  $-3^{\circ}\text{C}$  are more difficult to detect because there is less heat released on initial freezing and crystallisation happens over a longer period of time (see section 2.4). Manual inspection is required in this temperature regime and the  $2^{\circ}\text{C}$  threshold adjusted accordingly. ”

P7 L179-182: The authors may want to extend this part and explain the points more intuitively

We have rewritten this section to explain the process more clearly “Using the analysis code, an event is identified and recorded. The code then reads the temperature of the frame directly after this freezing event and calculates the difference of this value compared to  $0^{\circ}\text{C}$  to give an offset correction value, i.e. if the frame after freezing read  $2^{\circ}\text{C}$  then the correction factor for this well would be  $-2^{\circ}\text{C}$ . This offset value is then subtracted from all of the temperature recordings for that specific well. The average correction value calculated for the IR camera via this method is  $-1.9^{\circ}\text{C}$  with a standard deviation  $\pm 0.5^{\circ}\text{C}$ .”

P7 L189-192: The reviewer is curious if using different droplet volume can improve this uncertainty. The reviewer does not intend to ask any additional measurements (especially since  $\pm 0.9\text{ }^{\circ}\text{C}$  uncertainty is well justified in L193-207), but doe the authors have any estimates of the maximum/minimum droplet volume that IR-NIPI can deal with?

We have not completed any thorough experiments with different droplet volumes but the 96 multiwell plates can hold  $200\mu\text{L}$  droplets. The IR-NIPI should have no problem monitoring these volumes although the gradients within the wells will become larger. Volumes below  $50\mu\text{L}$ 's maybe possible but would be starting to come close to the limits of the IR cameras resolution. If the IR cameras resolution were to be improved then smaller droplet sizes should be possible.

P8 L214: Delete “see”.

Done

P11 L298-300:  $16.7\text{ L/min} * 100\text{ min} = 1670\text{ L}$ . . . The authors might want to check their nINP (L-1) since they might have employed a wrong Vs (Eqn. 2).

Thank you for noticing this. This was a typo and has now been corrected.

P11 L304: Was a dilution used to prepare suspensions for the ambient sample analysis? If not, no worries. But, if yes, the dilution factor is missed in Eqn. 2.

No dilution was used.

Fig. 7A: There seems some outliers within this  $T$ - $n_s(T)$  scale (i.e., 0.01 wt% run 2). What is responsible for them? Perhaps, it is due to what is addressed in L280-293? Please clarify.

We believe this may be related to the issues discussed in L280-293. We have added a sentence to emphasise this in the results discussion of Fig. 7A. “The  $n_s(T)$  values derived from IR-NIPI with 0.01, 0.1 and 1 wt% NX-illite are shown in 7a. They are in good agreement with one another with lower wt% suspensions yielding data at lower temperatures and higher  $n_s(T)$  values, as expected. The few data points from the 0.01wt% NX-illite run 2 which appear as outliers may indicate that the particles were not evenly distributed throughout the droplets.”

## Response to Referee #2

We would like to thank the referee for their insightful comments and have responded below. The referee comments are highlighted in red with our responses in black.

This manuscript presents a new instrument to measure low concentrations of ice nucleating particles in the atmosphere. It relies on commercial multiwell plates to allot the samples extracted from filters. For cooling, it uses a Stirling engine chiller that can be easily operated in the field. Because the heat transfer between the chiller and the multiwell plate is not uniform, the temperature of each well is determined with an IR camera. The same camera is also used to detect freezing from the heat release. To retrieve the actual temperature of the wells, use is made of the temperature increase upon freezing. The plateau temperature reached during freezing is taken as 0°C and the whole temperature curve is adjusted to this reference value by applying an offset correction. Validation and calibration revealed a temperature uncertainty of  $\pm 0.9^\circ\text{C}$ . The setup has been tested with K-feldspar chips, NX-illite and an aerosol sample taken from the City of Leeds. All these measurements show reasonable agreement with reference measurements from literature or performed with the  $\mu\text{L-NIPI}$  developed and available in the Leeds group. This manuscript is well suited for AMT and will be useful for other groups developing similar setups. For publication in AMT, the quality of presentation should be improved. Some descriptions remain vague and the figures are often not fully explained. In the introduction there is often only one reference given, while other relevant references to support the statements are lacking.

### Comments

Lines 22 – 23: “and their temperature is determined by the ice-liquid equilibrium temperature....” This sentence should be improved because it is difficult to understand without having read through the manuscript.

We have amended the text to read as “In this paper we first present the calibration of the IR temperature measurement, which makes use of the fact that following ice nucleation aliquots of water warm to the ice-liquid equilibrium temperature (i.e. 0°C when water activity is  $\sim 1$ ), which provides a point of calibration for each individual well in each experiment.”

Line 46: literature referring to more recently developed CFDC’s should be added.

References have been updated to: “There are several different methods of conducting ice nucleation experiments that include Continuous Flow Diffusion Chambers (CFDC’s) e.g. (Salam et al., 2006; Rogers et al., 2001; Kanji and Abbatt, 2009; Stetzer et al., 2008; Garimella et al., 2016; Kohn et al., 2016),

Line 56: Vergara-Temprado et al. (2017) is not the best reference to support this statement. Other references need to be added, e.g. Kanji et al. (2017).

Kanji *et al.* (2017) added. Vergara-Temprado et al. 2017 was a modelling study in which field data was compiled and compared to the model. One conclusion from this study was that there was a lack of field data.

Line 61: Again, this statement needs to be based on more and more recent literature because different types of CFDC’s are in use.

This has now been updated to include the following references “(Eidhammer et al., 2010; Al-Naimi and R., 1985; Prenni et al., 2009; DeMott et al., 2010)”

Line 61: the aerosol concentrator needs to be referenced.

Now referenced “This can be improved with aerosol concentrators (Prenni et al., 2013; Tobo et al., 2013),...”

Lines 64 – 66: “In principle, if the ice-nucleating properties of the aerosol particles in question are insensitive to mixing state, then increasing the amount of aerosol per droplet will scale with inverse proportionality to the INP concentration,...”. This sentence needs to be improved. What is meant by “mixing state” in this context? What is meant by “increasing the amount of aerosol per droplet will scale with inverse proportionality to the INP concentration?” Do you really mean “aerosol per droplet” or not rather “particles per droplet”?

This has now been reworded to “In principle, increasing the number of particles per droplet, and therefore surface area of nucleator per droplet, will increase the sensitivity of the experiment to rarer INP. This enables quantification of lower INP concentrations.”

Line 69: “volume of suspension used in each aliquot”: this formulation needs to be improved. The volume of suspension can be easily increased by diluting the suspension, but I guess this is not what is meant. Moreover, if filter samples are collected, it needs to be explained why extracting the filter with less water or evaporation of some of the water used for extraction is not an option.

We are not ruling out other methods of increasing the number of particles per aliquot of water, there may be other alternatives. We have focused on what we have done here. We have modified the section as follows: “The alternative approach is therefore to increase the number of particles within each aliquot of water. In principle, increasing the number of particles per droplet, and therefore the surface area of nucleator per droplet, will increase the sensitivity of the experiment to rarer INP. This enables quantification of lower INP concentrations” To increase the number of aerosol particles per volume of liquid the time period over which an atmospheric sample is collected can be extended, but in doing so temporal resolution would be lost. A method of increasing the sensitivity of an immersion mode technique is to increase the volume of the collected suspension used in each aliquot, while maintaining the concentration of particles per unit volume. This increases the number of particles per aliquot of liquid and therefore makes it more likely that rarer INP will be detected. The use of larger volume droplet suspensions has been exploited in the past e.g. (Vali, 1971; Bigg, 1953), and has been the strategy employed in the development of some recent instruments e.g. (Beall et al., 2017; Du et al., 2017; Stopelli et al., 2014; Conen et al., 2012). These large volume assays capture the rarer, more active INP but often miss the more abundant but less active INP. Hence they are frequently used alongside a smaller droplet instrument to achieve a complimentary dataset.”

Line 131: Where does the difference in set cooling rate and realized cooling rate come from? Why is this difference constant?

This cooling rate comes from a series of preliminary experiments with the justification being seen in the ramp rates for the IR-NIPI seen in the figures. The difference is likely constant as it is a lag between the temperature transfer from the cooled aluminium plate to the multiwell plate.

Line 152: What is meant by “aging of a sample in water”?

It has been demonstrated that for some materials ice-nucleating ability will change with time spent in water, sometimes over short periods of time. We have altered the text to clarify this and added references that demonstrate this behaviour. “This not only speeds up analysis, it also reduces the effect of any time-dependent aging processes such as the rapid deactivation of an albite sample suspended in water observed by Harrison et al. (2016).”

Lines 155 – 156: How representative is the surface temperature for the temperature distribution within the wells? Heat transfer simulations of Beall et al. (2017) performed for their multiwell setup showed temperature gradients within the wells. Please comment.

Yes, there are likely to be gradients in the wells, but our feldspar chip experiment suggest the gradients within the wells are not biasing results beyond the quoted uncertainty. The IR camera gave similar results to those of the  $\mu\text{l}$ -NIPI instrument where gradients in the droplet are thought to be negligible. In the IR-NIPI the feldspar chips are at the base of the well and our IR camera is reading the water air interface, yet we still see good agreement with the  $\mu\text{l}$ -NIPI system (within the T uncertainty).

It should also be noted that we did experiments with both polystyrene and polypropylene plates. Polypropylene is an order of magnitude greater thermal conductor than polystyrene. Between the two plates we saw no difference in freezing temperatures of NX-illite and the calculated offsets between the two experiments were similar (within the  $0.6^{\circ}\text{C}$  standard deviation mentioned earlier). Hence, we again think that the gradients are minor in all cases.

We think this is discussed adequately in section 3.3.

Lines 164 – 165: The increase of the well temperature up to  $0^{\circ}\text{C}$  during freezing indicates a slow heat removal and limited thermal contact to the aluminum cold stage via the thermally conductive pad. From this, heating of adjacent wells is expected. Can you comment on this?

We expect to see a rise in temperature to equilibrium irrespective of thermal contact. The heat production during the initial crystal growth process is very rapid, much more rapid than the rate at which heat is dissipated for almost all droplet arrays even in  $\mu\text{L}$  droplets on an aluminium block. We do expect to see some heating of neighbouring wells but it is often minor and we do not have any quantitative data to describe the extent of this heating. However, you can see an example of the heating of neighbouring wells in Fig. 4A at  $\sim 2000$  seconds where a well has frozen and the neighbouring wells increase in temperature. The use of individual temperature measurements of wells mitigates any impact this heating might have on freezing temperatures. In the caption we have added 'Note that the freezing events at  $\sim 2000$ s appear to cause some heating in the adjacent well.'

**Line 168: how can you observe that the temperature maximum was reached within 1 s when you read out the IR camera only every 20 s? What do you mean by visual inspection?**

We record an image every 20 seconds but the IR camera we use has a live screen display in which we can monitor the experiment. The text has been altered to reflect this "Visual inspection of the live screen display of the IR camera revealed that the temperature reached a maximum within 1 s."

**Line 173: Can you quantify the temperature differential between the cold stage and the aliquot?**

We know that the cold plate is significantly colder than the water aliquots. This does not matter because we use the IR emissions to monitor temperature. As explained in the text the ramp rate is set to  $1.3\text{ }^{\circ}\text{C min}^{-1}$  (which results in a cooling rate of  $1\text{ }^{\circ}\text{C min}^{-1}$  in the aliquot) to account for a lag between the cold stage and aliquot. We do not think there is a need to quantify the offset of the cold stage and the aliquot any further as we measure temperature independently via the IR camera.

**Lines 183 – 186: You mention several aluminum wells. How many did you test?**

We used 16 in an experiment but only monitored 3 of them with thermocouples. This is now explained in the text: "We performed a number of experiments to test the IR temperature measurement calibrated using the above method. In the first instance we used highly conductive individual anodised aluminium wells for  $50\mu\text{L}$  droplets. The temperatures of three of these wells were recorded independently using T type thermocouples embedded in the aluminium wells to give a representative temperature of the well and aliquot of water (see inset in **Error! Reference source not found.**)"

**Lines 196 – 198: It would be helpful if you could add a figure illustrating the temperature gradient within the plate**

The temperature gradient can be seen in figure 2a. This is now referenced in the text "As mentioned above there is a gradient across the entire plate (Fig. 2A)..."

**Lines 204 – 205 and Fig. 4: From the scheme shown in the inset, results from 12 wells should have been measured, but in Fig. 4B results of only 6 wells are shown. Why? It would be helpful when you would label the wells shown in the inset with the numbers of the wells indicated in panel B.**

Two wells measured with thermocouples were contrasted to three surrounding wells measured with the IR camera, so a total of six IR measurements were recorded. The schematic inset was to demonstrate that thermocouples were placed in the corners where the difference between the surrounding wells was at a minimum and that up to four of the surrounding wells could be used to compare to the thermocouple measured well. We accept the schematic is confusing and has been redrawn just to display the position of the wells observed.

**Lines 215 – 216: By how many degrees was the freezing temperature reduced due to filtering of the Milli-Q water?**

It looked to improve the baseline by  $\sim 2\text{-}3^{\circ}\text{C}$ . This has been added to the text. "Filtering of the Milli-Q water to  $0.2\text{ }\mu\text{m}$  reduced the temperature at which pure water droplets froze by  $2\text{-}3^{\circ}\text{C}$ . Sartorius Ministart, non-pyrogenic, single use filters were used for this (product code 17597-K)."

**Section 3.3 and Fig. 6 (Feldspar chips): This section needs better explanations of the rationale and the execution of the experiment.**

We have made section 3.3 clearer.

- You refer to Whale et al. (2015) for the setup but Whale et al. describes experiments with droplets containing a suspension of mineral particles and not with grains/chips. Please explain better the sample preparation of this study.

The reference in the text is for Whale *et al.* (2018) in which they describe this method. We later reference Whale *et al.* (2015) for the later stages of the experiment as the overall procedure of the experiment is explained better in this paper. This is clearer now in the revised section.

- How large were the grains/chips?

This is in the text as “each droplet contained a single ~100  $\mu\text{m}$  sized grain of K-feldspar” but has been re-clarified later in the text as “A total of 19 grains were collected (~100  $\mu\text{m}$  in size), assigned a number and their position tracked through the course of each experiment.”

- How many droplets were deposited on a grain for the  $\mu\text{L}$ -NIPI experiment?

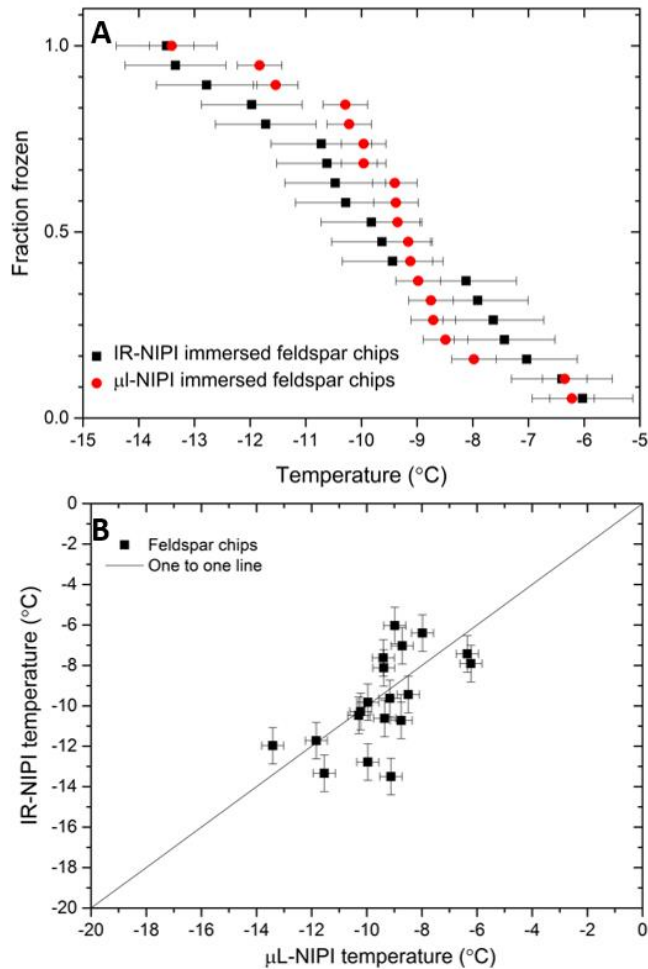
A single  $\mu\text{L}$  droplet was deposited on top of each grain. This has now been clarified in the revised text. “The grains were then used in the  $\mu\text{L}$ -NIPI experiment by placing the grains onto a glass cover slip atop a cold plate and pipetting a single 1  $\mu\text{L}$  droplet onto each grain, before carrying out a standard  $\mu\text{L}$ -NIPI experiment.”

- Are the results shown in Fig. 6 averages from all 20 selected grains? The “fraction frozen” label on the y-axis seems to indicate this. If yes: why did you select 20 individual grains if you lump all results together in the end?

The grains have not been averaged. Each droplet in the experiment contains a single grain and so there is a single freezing temperature recorded for each grain. The plot is showing the fraction frozen.

- You show 19 IR-NIPI (black squares) and 19  $\mu\text{L}$ -NIPI (red circles) data points. Is there a correspondence with the individual chips? Is on each line of the plot a pair of IR-NIPI and  $\mu\text{L}$ -NIPI results of the same chip? If this is the case, the labeling of the y-axis as fraction frozen is misleading. Rather, in this case, the y-axis should indicate a numbering of the grains.

We have include a separate plot in fig 6 to demonstrate this. We have now plotted IR-NIPI freezing temperature for a feldspar chip against the freezing temperature measured on the  $\mu\text{L}$ -NIPI. The one to one line is displayed along with the error in temperature for the two instruments. This can be seen in figure 6 below.



We have revised the text to the following in section 3.3: “The resulting fraction frozen plot for this experiment can be seen in Figure 2a and the corresponding correlation plot is shown in Figure 6b. The two instruments yielded similar fraction frozen curves and the individual feldspar grains nucleated ice at a similar temperature in both experiments. The correlation plot in Figure 6b shows that the freezing temperatures of a single grain were not identical in the two experiments, which is consistent with the stochastic nature of nucleation at active sites that have a characteristic freezing temperature (Vali, 2008; Vali, 2014). The agreement between the two instruments suggests that the temperature measurement and calibration of the IR-NIPI were robust and that there is no major temperature gradient within the aliquots in the multiwell plates.”

The caption has also been updated to “**Figure 1. (A)** Plot of the fraction frozen curves for single feldspar particles per droplet in both the  $\mu\text{L-NIPI}$  (using 1  $\mu\text{L}$  droplets) and  $\text{IR-NIPI}$  (using 50  $\mu\text{L}$  droplets) experiments. The error bars display the error in temperature measurement on both instruments. **(B)** Shows the freezing temperature for the individual feldspar chips as measured by the  $\text{IR-NIPI}$  and  $\mu\text{L-NIPI}$  instruments. The one to one line is shown in bold and the error in temperature for the two instruments are represented by the error bars.”

Why 19 and not 20 data points when you chose 20 grains?

This is a typo. We originally had 20 grains but one grain was dropped whilst transferring it over to the next experiment so only 19 grains were tested on both experiments. We have changed 20 to 19 in the text.

• What is the meaning of the error bars? Did you perform several freezing cycles and average? Did you average over several droplets on top of a grain in the case of  $\mu\text{L-NIPI}$ ?

The Error bars are simply the errors associated with the temperature measurement. This has now been clarified in the figure caption. “**Figure 2.** Plot of the fraction frozen curves for single feldspar particles per droplet in both the  $\mu\text{L-NIPI}$  (using 1  $\mu\text{L}$  droplets) and  $\text{IR-NIPI}$  (using 50  $\mu\text{L}$  droplets) experiments. The error bars display the error in temperature measurement on both instruments.”



- In some cases the error bars of IR-NIPI and  $\mu\text{L}$ -NIPI do not overlap. Any explanation?

This is consistent with the stochastic nature of nucleation at active sites. This is now discussed in the revised section 3.3.

- It is unclear why chips are taken and not suspensions with concentrations adjusted such that the mass of K-feldspar is the same for the 1  $\mu\text{L}$  drops of the  $\mu\text{L}$ -NIPI and the 50  $\mu\text{L}$  drops in the multiwell plate of the IR-NIPI setup.

We have improved the motivation of section 3.3. We have now added the following text “The purpose of this experiment was to have the same amount of material per droplet in each experiment and to have the material at the base of the droplet in order that the results from the two instruments could be directly compared. In doing so we could investigate the extent to which the gradient within the 50  $\mu\text{L}$  wells might be a problem.”

Line 259:  $n_s(T)$  should be the same independent of concentration because it refers to one temperature and is per illite surface area present in a sample.

When we change the surface area of material in a droplet we change the  $n_s$  to which we are sensitive. We have modified the text to refer to surface area instead of wt% suspensions to help minimise confusion. “The results demonstrated good agreement with each other and exhibited the expected trend of the droplets containing smaller amounts of nucleant surface area freezing at lower temperatures and having higher  $n_s(T)$  values than the droplets with higher amounts of surface area.”

Line 300: 167 L: shouldn't 16.7 x100 yield 1670 L?

This was a typo and has now been changed to 1670

Line 300: Why is “filters” in plural? How many filters did you collect and measure?

One sample was collected and referred to here. Others were collected, but these will appear in a separate publication. The text has been altered to reflect this. “In order to demonstrate the utility of this approach for atmospheric aerosol samples, a filter sample was collected in Leeds as part of a field campaign held on the evening of the 5<sup>th</sup> November. A sample of atmospheric aerosol was collected using a Mesa PQ100 air sampler for 100 min. An inlet head with an upper cut-off of 10 $\mu\text{m}$  was utilised and air was sampled at 16.7 L  $\text{min}^{-1}$  on to a 0.4  $\mu\text{m}$  polycarbonate track-etched Whatman filter, with a total of 1670 L of air sampled. The filter was then placed in to 6 mL of Milli-Q water and vortexed for 5 min to wash the particles from the filter and into suspension.”

Line 310: specify what kind of modelling you mean here.

The text has been modified to “Since high-resolution regional modelling of the effect of INP on high latitude, cold sector-clouds suggests that 0.1 to 1 INP  $\text{L}^{-1}$  is a critical concentration and much lower concentrations still impact clouds (Vergara-Temprado et al., 2018), measurements with IR-NIPI will be extremely useful, particularly in environments with low INP concentrations.”

Lines 317 – 318: this formulation should be improved

The text has been adjusted to “We demonstrate that IR thermometry is a sound method for determining the freezing temperature of 50  $\mu\text{L}$  water droplets in multiwell plates. This method overcomes potential distorting influences such as thermal gradients across the plate, the effect of freezing wells warming surrounding wells and poor thermal contact to the underlying cold plate.”

Line 333: Could you specify here how you intend to automate the system further.

We have ideas for the potential automation but would rather not specify them here. We realise this comment is vague and so have removed the following sentence from the text. “The use of the multiwell plates and the IR camera lends the IR-NIPI to the possibility of automating the system further and this is an objective for future work.”

Figure 1: can you indicate in this figure how the Stirling engine chiller is connected to the aluminium cold stage?

The figure has been adjusted to show this. Please see below.

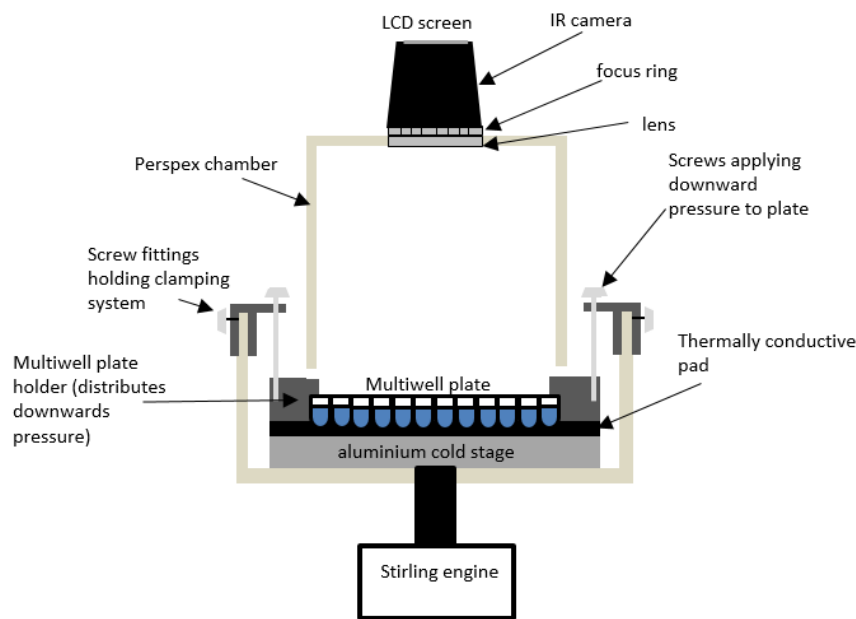


Figure 2B: one temperature ramp seems to be an outlier to warmer temperature. Do you know why?

We think the well associated with this temperature ramp had poor thermal contact with the underlying pad. An advantage of using the IR measurement of each well is that the influence of such issues is removed. The following has been added to the caption: “Note that one well had a higher temperature than the others, likely due to poor thermal contact with the aluminium substrate. By using IR thermometry to measure the temperature of each well individually such variability is accounted for.”

Figure 3, inset: the water in the aluminum well is drawn as if it did not wet the well. Is this realistic? Was the aluminum coated?

The aluminium was anodised and was hydrophobic, hence this is realistic.

Figure 3, the figure caption of panel B needs to state explicitly whether  $T(\text{thermocouple}) - T(\text{IR})$  is shown or the opposite. You might discuss the implications of the negative peaks observed in the residuals of panel B.

This has been clarified in the figure caption “The difference was calculated by  $\text{IR}(T) - \text{Thermocouple}(T)$ . The negative spikes are a result of the IR camera directly reading the water temperature as it is heated by ice formation whereas the thermocouple measurement is reading the temperature of the aluminium well which is less affected by the latent heat release.”

Figure 3, figure caption, line 523: “The point of freezing is highlighted in blue”... This statement is confusing since a whole area is indicated in blue. Do you mean “the area of freezing” or to which point do you refer?

This has now been corrected to “The range over which freezing occurs is highlighted with a blue rectangle as this is where the thermal properties of ice and the initiation of heat release affect the temperature readings.”

Figure 4, figure caption, line 542: “A schematic diagram of the experiment is shown of the wells within a 96 well plate chosen for temperature checks.” This sentence needs to be improved.

The text has been modified to read “A diagram of the wells within a 96 well plate chosen for the comparison of IR and thermocouple measurements is displayed as an inset.”

Figure 4, the figure caption of panel B needs to be improved. Which wells are shown? Can you number the wells in the multiwell plate shown as an inset in panel A according to the numbering in panel B?

This is a good idea, we have adjusted the inset to correspond to the numbers in panel B and amended the figure caption accordingly. Please see below.

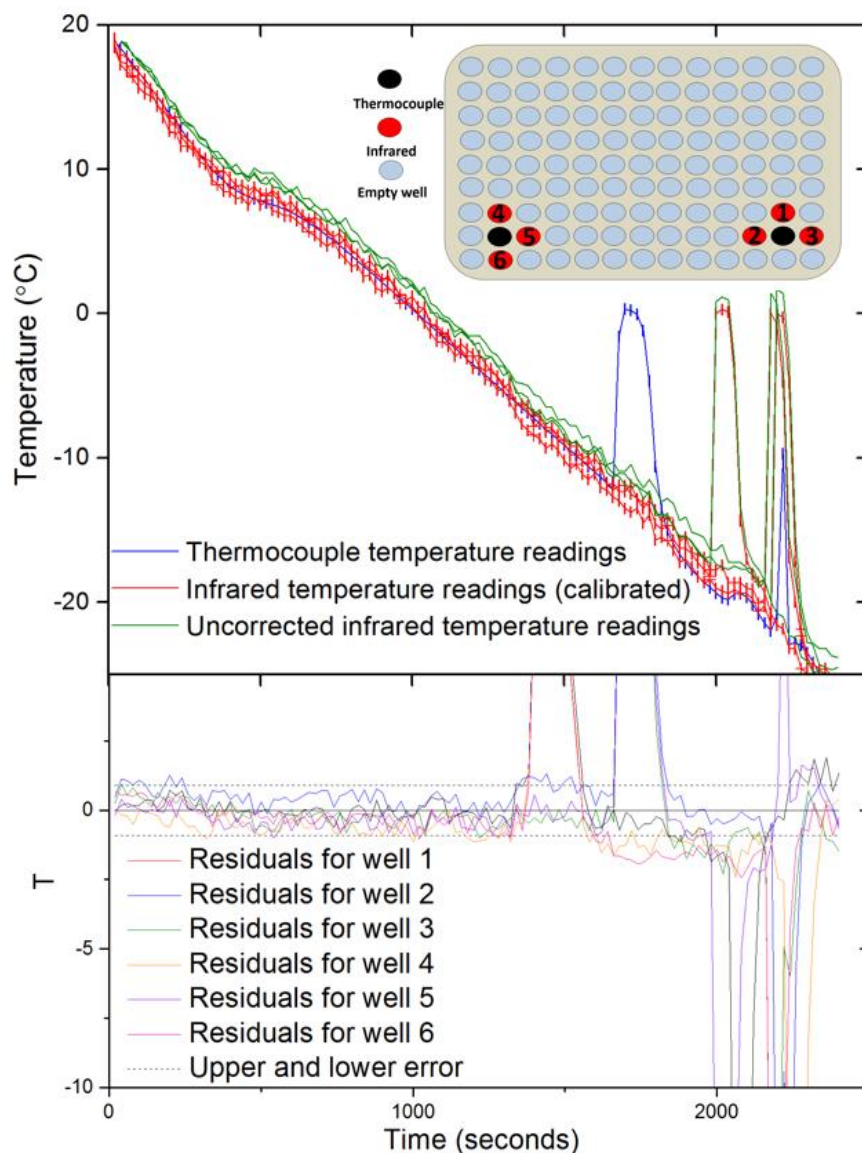


Figure 5: the y-axis has a strange scale with 5 digits between labels, implying a spacing of 0.08333333?!?! You might want to improve.

Thank you for pointing this out. It has now been adjusted to 0.1 increments.

Figure 5: the different blank curves should be given with different colors or symbols so that they can be discriminated from each other. For some blanks, the data points at low fraction frozen seem to be missing!?

We have created 3 separate panels for this figure to show the corresponding internal blanks with the relevant experiments. The main/original plot shows a culmination of representative blanks from this set up. The data points at low fraction frozen are not missing for the blanks. For the internal water blanks 12 wells were dedicated to a handling blank, hence the lower data density compared to blanks where we used all of the wells to test the water quality.

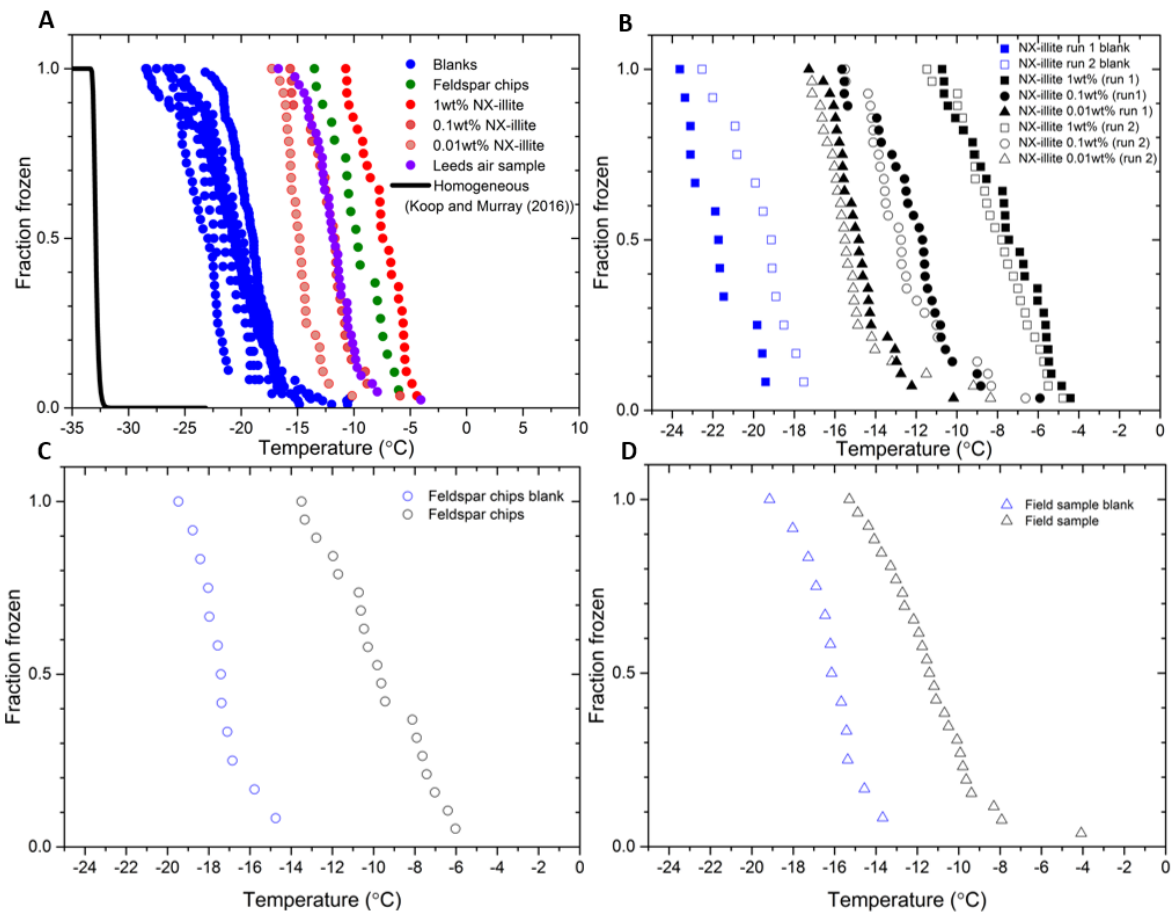


Figure 7A: The two darker blues and the two darker reds are difficult to discriminate. Please improve the color palette.

This has now been amended.

Figure 7A, figure caption: the error bars should be explained. Is this the error of  $\pm 0.9^\circ\text{C}$  or the standard deviation between several freezing cycles?

The figure caption has been amended to address this. “The error bars represent the temperature error of  $\pm 0.9^\circ\text{C}$ .”

**Technical comments**

Line 49: “systems” should be replaced by “methods”

Done

Lines 73 – 75: “This instrument is part of the NIPI suite of instruments that includes the  $\mu\text{L}$ -NIPI and when used together these devices allow measurements to be taken over a very wide range of INP concentrations.” Consider splitting this sentence into two

Changed to “This instrument is part of the NIPI suite of instruments that includes the  $\mu\text{L}$ -NIPI. When used together these devices allow measurements to be taken over a very wide range of INP concentrations.”

Line 92: what is meant by “other expressions”?

Changed to “The fraction of the droplet population frozen throughout the explored temperature range can then be determined, from which the ice-nucleating active site density or INP concentration can be derived (Vali et al., 2015).”

Line 130: “Stirling engine chiller” would be more precise.

This has been changed to “The unique design, in combination with a Stirling engine-based chiller...”.

Lines 156 – 158: the wording of this sentence should be improved.

This has been adjusted to “This contrasts with the approaches adopted in other experiments where the temperature is recorded and assumed to be representative for all droplets, for example when employing a cold stage housing an embedded thermocouple whose reading is used to represent the temperature of the droplet array.”

Line 214: remove “see”.

Done

Line 220: The reference “Polen et al., 2018” is missing from the reference list.

Corrected

Line 269: delete “and is illustrated”

Done

Line 271: “takes advantage” sounds strange. Try rewording.

This has been reworded to “This material has also been investigated by Beall *et al.* (2017) using an instrument that also uses 50 $\mu$ L droplets: the Automated Ice Spectrometer (AIS).”

Line 274: “were”: you switch to past tense here, while before you used present time.

The text has been altered to be in present. “Both the IR-NIPI and AIS data are in good agreement with one another. It can be seen that the larger volume assays (IR-NIPI and AIS) give results towards the upper spread of literature data but are still consistent with other results (**Error! Reference source not found.**b). Dry dispersed techniques have also been plotted as unfilled blue squares in Fig. 7b, but none of these techniques are sensitive in the range of  $n_s(T)$  seen by the large droplet instruments. The new data from the IR-NIPI has extended the dataset for NX-illite to warmer temperatures than in previous measurements, illustrating the utility of the technique.”

Line 281: “flowing”: do you mean “following”?

Yes, thank you. This has been changed.

Line 288: “suspended” instead of “suspend”.

Done

Line 300: “in to” should be one word.

Done

Line 305: in the equation it is “Nu(T)” not “Nυ(T)”. Please adjust.

Done

Lines 328 – 329: “an aerosol sample in the atmosphere of the city of Leeds” sounds strange. Improve formulation to e.g.: “an aerosol sample from the City of Leeds”.

This has been amended to “The utility of IR-NIPI for the analysis of atmospheric samples was also demonstrated by collecting and analysing an aerosol sample from the city of Leeds, England.”

Line 453 – 454: use abbreviation: Atmos. Chem. Phys.

Done

Legend of Fig. 6: “IR-NIPI” not “IR-NIP”

Thank you. This is now fixed

## **Response to Referee #3**

We would like to thank the referee for their insightful comments and have responded below. The referee comments are highlighted in red with our responses in black.

This is a well-written paper with an interesting experimental approach that fits perfectly well into the journal *Atmospheric Measurement Techniques*. The authors describe an instrument for quantifying heterogeneous ice nucleation: the InfraRed-Nucleation by Immersed Particles Instrument (IR-NIPI). They use multiwell plates and an infrared camera for detection of the freezing process. For comparison, they have investigated homogeneous ice nucleation of ultrapure water, and the heterogeneous freezing of two mineral dust samples. The manuscript should be published in *AMT* after major revisions.

### **Comments**

In line 72, the authors claim “Here we propose a new technique, . . .”. Unfortunately, this is not entirely true. A quick literature research shows that there are other instruments with very similar approaches. In particular, I would like to mention the set-ups of Zaragotas *et al.* and of Kunert *et al.* It is good scientific practice to search, to describe, and to discuss the findings of other scientists when presenting a new set-up. I expect that the authors make up the leeway in the revised version of the manuscript. Concerning the set-up of Kunert *et al.*, I could not find any peer-reviewed publication, but I have been the organizer of two ice workshops (Kunert 2016b, 2017b) and the convener of two EGU General Assembly sessions (Kunert 2016a, 2017a) and a speaker at the INUIT Final Conference and 2nd Atmospheric Ice Nucleation Conference (Kunert 2018), where this research has been presented. At all these meetings, also the authors were present and in the case of the latter have even been the organizers. Therefore, the Twin-plate ice nucleation assay (TINA) with infrared detection by Kunert *et al.* is well-known to them and should be described in their manuscript for comparison with IR-NIPI.

The omission of Zaragotas *et al.* (2016) was a major oversight and we thank the reviewer for bringing this to our attention. The instrument discussed is applied to the cryobiology field but is a similar set up to the IR-NIPI and supports the use of IR cameras for this application.

With regards to the various conference presentations made by Kunert *et al.* there was no peer reviewed literature for this technique at the time of submission and hence it was not cited or discussed. However on the 24th of July Kunert *et al.* have had a publication accepted for review and posted on the *AMT* discussion forum. We are then happy to include this reference and have altered the text to include it.

We have included the references to these papers in sections 1 and 2.4.

In section 1: “While many instruments use optical cameras to detect freezing events (Whale *et al.*, 2015; Budke and Koop, 2015; Häusler *et al.*, 2018; Beall *et al.*, 2017), some researchers have used techniques to detect the release of latent heat associated with freezing. For example differential scanning calorimetry (Marcolli *et al.* 2007; Pinti *et al.* 2012) and infrared emissions (Zaragotas *et al.*, 2016; Kunert *et al.* 2018) have been used. Zaragotas *et al.* (2016) use a thermal camera to measure the temperature of individual aliquots within a 96 multiwell plate partially submerged within an alcohol bath. This study investigated plant samples but suggested that the technique may be adapted for atmospheric purposes. Very recently, Kunert *et al.* (2018) presented a similar set up to investigate biological samples and collected aerosol. Unlike Zaragotas *et al.* (2016), Kunert *et al.* (2018) do not measure individual droplet temperatures via infrared emissions but instead use multiple thermistors embedded in the sample holders to infer temperature for the droplet array.”

In section 2.4: “It should be noted that one of the limitations of the setup used by Zaragotas *et al.* (2016) was that the IR camera was calibrated only once by the factory, however our calibration method mitigates this limitation.”

In line 48, the authors list some droplet freezing assay experiments but the list is rather incomplete, e.g. Häusler 2018 is missing. I strongly recommend a table with all technical parameters of each experiment listed, e.g. number of observed volumes, volume of the droplets, homogeneous ice nucleation temperature, etc. Finally, for all experiments a discussion of the pros and cons in comparison to IR-NIPI should be added.

This list was not intended to be exhaustive, but representative. We have now added the reference of Häusler *et al.* (2018) to the list of drop assay references.

We think that a table reviewing all previous droplet freezing assays is beyond the scope of this techniques paper. A table of such a nature would be much better suited in a review or intercomparison paper. There are papers already available which describe such advantages and disadvantages of the various styles of instruments and are referenced in the text “For more information on the capabilities and limitations of the various techniques see the comprehensive reviews and intercomparisons conducted by Hiranuma *et al.* (2015) and (DeMott *et al.*, 2018). Häusler *et al.* (2018) also presents a summary of the features of various techniques.”. In addition, we are aware of a paper describing many techniques from the FIN02 activities which has recently been submitted to AMTD and added to the references in text.

Instead, the authors compare only their own set-ups, i.e.  $\mu\text{L-NIPI}$  and  $\text{IR-NIPI}$ . However, the volume of the respective droplets is very different,  $1\mu\text{L}$  versus  $50\mu\text{L}$ , respectively.

We have compared a wide variety of different techniques when investigating the NX-illite sample. We chose NX-illite as it allowed a direct comparison to literature data of a similar experiment in terms of droplet volume (the AIS instrument) as well as a wide range of other instruments (Hiranuma *et al.*, 2015). This included a direct comparison to another technique using  $50\mu\text{L}$  droplets (AIS). It should be noted there is limited literature data for  $50\mu\text{L}$  droplets and NX-illite is the only material we can compare directly to as a result of this. We compared to our  $\mu\text{L-NIPI}$  technique for other samples, because this is available in our laboratory and we could operate the two instruments side by side with the same sample.

This is not only important for homogeneous ice nucleation, which shows strong volume dependence, but also is important for heterogeneous ice nucleation because larger volumes carry more INPs and the abundance of efficient INPs rises. The authors have discussed this only partly and a more elaborated discussion might be necessary.

The text has now been amended to expand on this topic to read “The alternative approach is therefore to increase the number of particles within each aliquot of water. In principle, increasing the number of particles per droplet, and therefore the surface area of nucleator per droplet, will increase the sensitivity of the experiment to rarer INP. This enables quantification of lower INP concentrations” To increase the number of aerosol particles per volume of liquid the time period over which an atmospheric sample is collected can be extended, but in doing so temporal resolution would be lost. A method of increasing the sensitivity of an immersion mode technique is to increase the volume of the collected suspension used in each aliquot, while maintaining the concentration of particles per unit volume. This increases the number of particles per aliquot of liquid and therefore makes it more likely that rarer INP will be detected.”

In particular, I miss plots of the homogeneous freezing events and a detailed study of the freezing of single droplets (marked with numbers on a picture of the multiwell assay). I also recommend adding the diameter of the droplets to the volume to make the study more comparable to other studies.

We are unable to reach homogenous in this setup, as with all techniques employing such large droplets. The expected homogeneous curve can be seen in figure 5 and our blanks are well above this. We do not see the value of numbering specific droplets in an array, this is not information we routinely collected.

Our droplets are not spheres in the multiwell plates so a diameter is not relevant but we have quoted a volume equivalent diameter to help compare to other studies. “The most useful for this freezing assay are the  $96 \times 200\mu\text{L}$  or  $384 \times 50\mu\text{L}$  aliquot arrays and in the tests reported here  $50\mu\text{L}$  droplets ( $\sim 2300\mu\text{m}$  volume equivalent diameter) are used in 96 well plates.”

The authors make the point that their set-up is more sensitive for low concentrations of INPs, which is particularly true for strong INPs. However, they don't mention the disadvantage of their set-up, which is that they cannot easily measure weak INPs. In the atmosphere, the number of strong INPs is extremely low, which makes  $\mu\text{L-NIPI}$  a valuable technique. However, often strong INPs are entirely missing and weak INPs will be much more abundant. Therefore, the authors should discuss the limitations of their set-up and should also show experiments at the detection threshold and should investigate proxies for weak INPs e.g. cellulose or soot.

We have now tried to clarify the point that the  $\text{IR-NIPI}$  instruments compliment smaller droplet techniques. The section of text added reads “These large volume assays capture the rarer, more active INP but often miss the

more abundant but less active INP. Hence they should ideally be used alongside a smaller droplet instrument to generate complimentary datasets.”

Also I miss biological INPs or proteins and polysaccharides been emitted by biological sources. Therefore, beside ns values of solid INPs also nm values of soluble INPs should be measured and discussed.

We accept that this would be interesting to investigate but again believe it is beyond the scope of this paper which is to outline the concept of the technique. We have some interesting results from biological materials and would like to use these in another paper and do not think this is the best place to present this data. We believe that we have already provided sufficient examples of materials used in the IR-NIPI system.

## Specific comments

Where is the homogeneous freezing temperature (T50) of ultrapure water in your IRNIPI set-up?

Homogenous freezing (T50) for 50 $\mu$ L droplets is  $\sim$ -32.5°C based on Murray and Koop (2016). This is presented in figure 5. We have not accessed homogeneous freezing and do not claim to do so.

Line 99: Also indicate the formula for nm and add respective water soluble samples.

We do not think this is necessary as explained above.

Line 182: “standard deviation  $\pm$ 0.5°C”

Thank you. This has been changed.

Line 190: “after the first equilibrium step at +5°C”

Thank you. This is changed to the suggested.

How is the temperature uncertainty in the range between -20° and -30° C?

We are unable to quantify the uncertainty as the thermocouples and water often freezes before this point but we assume that it is similar to that stated for the temperature range above -20°C. We are mainly interested in the temperature of samples above -20°C as below this we enter our baseline. The uncertainty within this temperature range is of secondary importance for our experiments.

You have only used ultrapure water for temperature calibration. How about other samples such as aqueous salt solutions, higher alcohols or alkanes?

As you have rightly pointed out we have only calibrated on the basis of ultrapure water. We have done this because we are only using water suspensions and have not attempted to study nucleation in different solutions or other materials. Furthermore, using solutions or other liquids for a calibration would not be applicable for water, since they have different thermal conductivities and different thermal emissivity. The IR camera is already corrected based on the thermal emissivity of water and hence using other solutions or liquids would introduce new errors.

Line 215: What kind of filter has been used for purification?

Thank you for highlighting this. It has now been added to the text. “Sartorius Ministart, non-pyrogenic, single use filters were used for this (product code 17597-K).”

A figure, similar to that in fig. 7B, should be plotted also for feldspar samples including comparison data from other groups.

We believe that is not needed for this paper as for the same reasons as mentioned earlier. We believe we have already demonstrated the use of the IR-NIPI with sufficient materials and that this would be more applicable for an intercomparison paper and has been done so by DeMott *et al.* (2018). In addition there is also no published literature data for feldspar in the droplet regime for the IR-NIPI so no direct comparison can be made. This was one of the reasons we chose to include a comparison with NX-illite.

In figures 2, 3, 4, and 7 capital letters have been used in the graph but small letters have been used in the figure caption, respectively.

Thank you. This has been amended.





1 **An instrument for quantifying heterogeneous ice nucleation in multiwell**  
2 **plates using infrared emissions to detect freezing**

3  
4 **Alexander D. Harrison<sup>1</sup>, Thomas F. Whale<sup>1</sup>, Rupert Rutledge<sup>2</sup>, Stephen Lamb<sup>2</sup>, Mark D. Tarn<sup>1</sup>, Grace**  
5 **C. E. Porter<sup>1</sup>, Michael Adams<sup>1</sup>, James B. McQuaid<sup>1</sup>, George J. Morris<sup>2</sup> and Benjamin J. Murray<sup>1</sup>**

6 <sup>1</sup>School of Earth and Environment, University of Leeds, Leeds, LS2 9JT

7 <sup>2</sup>Asymptote Ltd., GE Healthcare, Sovereign House, Cambridge, CB24 9BZ

8 *Correspondence to:* A. D. Harrison (ee11ah@leeds.ac.uk) and B. J. Murray (b.j.murray@leeds.ac.uk)

9 **Abstract**

10 Low concentrations of ice nucleating particles (INPs) are thought to be important for the properties of mixed-  
11 phase clouds, but their detection is **challenging**. Hence, there is a need for instruments where INP concentrations  
12 of less than 0.01 L<sup>-1</sup> can be routinely and efficiently determined. The use of larger volumes of suspension in drop  
13 assays increases the sensitivity of an experiment to rarer INPs or rarer active sites due to the increase in aerosol  
14 or surface area of particulates per droplet. Here we describe and characterise the InfraRed-Nucleation by  
15 Immersed Particles Instrument (IR-NIPI), a new immersion freezing assay that makes use of IR emissions to  
16 determine the freezing temperature of individual 50µL droplets each contained in a well of a 96-well plate. Using  
17 an IR camera allows the temperature of individual aliquots to be monitored. Freezing temperatures are determined  
18 by detecting the sharp rise in well temperature associated with the release of heat caused by freezing. In this paper  
19 we first present the calibration of the IR temperature measurement, which makes use of the [fact that following ice](#)  
20 [nucleation, aliquots of water warm to the ice-liquid equilibrium temperature \(i.e. 0°C when water activity is ~1\),](#)  
21 [which provides a point of calibration for each individual well in each experiment.](#) We then tested the temperature  
22 calibration using ~100 µm chips of K-feldspar, by immersing these chips in 1 µL droplets on an established cold  
23 stage (µL-NIPI) as well as in 50 µL droplets on IR-NIPI; the results were consistent with one another indicating  
24 no bias in the reported freezing temperature. In addition we present measurements of the efficiency of the mineral  
25 dust NX-illite and a sample of atmospheric aerosol collected on a filter in the city of Leeds. NX-illite results are  
26 consistent with literature data and the atmospheric INP concentrations were in good agreement with the results

**Commented [AH1]:** Deleted While instruments to quantify INPs online can provide relatively high time resolution data, they typically cannot quantify very low INP concentrations. Furthermore, typical online instruments tend to report data at a single defined set of conditions.

**Deleted:**

**Deleted:** T

**Deleted:** freezing

**Moved (insertion) [1]**

**Deleted:** the

**Deleted:** ,

**Deleted:** freezing period after initial nucleation. The difference in temperature of the point after initial freezing and the ice-liquid equilibrium temperature,

**Moved up [1]:** i.e. 0°C when the water activity is ~1,

**Deleted:** is used as an offset correction factor for calibration.

38 from the  $\mu\text{L-NIPI}$  instrument. This demonstrates the utility of this approach, which offers a relatively high  
39 throughput of sample analysis and access to low INP concentrations.

## 40 1 Introduction

41 Cloud droplets can freeze homogeneously below about  $-33^\circ\text{C}$  (Herbert et al., 2015), but the presence of ice-  
42 nucleating particles (INPs) can induce freezing at much warmer temperatures (Kanji et al., 2017). The glaciation  
43 of clouds at these warmer temperatures has a substantial impact on a cloud's reflective properties, lifetime and  
44 therefore the overall climate of the planet, but is poorly represented in many models (Hoose and Möhler, 2012;  
45 Vergara-Temprado et al., 2017). INPs can cause nucleation through a number of pathways (Vali et al., 2015), but  
46 in mixed-phase clouds it is thought that the pathways where particles become immersed in droplets is most  
47 important (Hande and Hoose, 2017; Hoose et al., 2010; Murray et al., 2012). Even small concentrations of INPs  
48 can influence cloud properties; for example, in a modelling study of Southern Ocean shallow mixed-phase clouds,  
49 Vergara-Temprado et al. (2018) showed that while concentrations of INPs greater than  $\sim 1 \text{ L}^{-1}$  cause profound  
50 changes in cloud properties, clouds are sensitive to concentrations many orders of magnitude smaller.

51 The ability to quantify INP spectra (INP concentrations as a function of temperature) and test the efficiency of  
52 proxy materials for ice-nucleating efficiency is invaluable for improving our understanding of cloud glaciation  
53 and developing computationally inexpensive parameterisations for atmospheric models. However it is not a trivial  
54 task, in part because INP concentrations are low ( $< 0.1 \text{ L}^{-1}$ ) (DeMott et al., 2010) and the sites on the surfaces which  
55 cause nucleation at warm temperatures (Vali, 2014; Whale et al., 2017) are rare. There are several different  
56 methods of conducting ice nucleation experiments that include Continuous Flow Diffusion Chambers (CFDC's)  
57 e.g. (Garimella et al., 2016; Kanji and Abbatt, 2009; Kohn et al., 2016; Rogers et al., 2001; Salam et al., 2006;  
58 Stetzer et al., 2008), cloud expansion chambers e.g. (Cotton et al., 2007; Niemand et al., 2012), wind tunnels e.g.  
59 (Diehl and Mitra, 1998; Pitter and Pruppacher, 1973) and droplet freezing assays e.g. (Beall et al., 2017; Budke  
60 and Koop, 2015; Häusler et al., 2018; Knopf and Alpert, 2013; Murray et al., 2011; Vali, 2008; Whale et al.,  
61 2015). Each of these methods has its limitations and advantages which must be understood and accounted for  
62 when conducting an experiment and interpreting the results. For example CFDCs cannot be used for  
63 measurements at temperatures warmer than about  $-11^\circ\text{C}$  but they do allow for specific saturation conditions to be  
64 controlled, something which other instruments cannot achieve. For more information on the capabilities and  
65 limitations of the various techniques see the comprehensive reviews and intercomparison<sub>s</sub> conducted by Hiranuma

**Deleted:** (Herbert et al., 2015){Herbert, 2015 #4194}

**Deleted:** developing computationally inexpensive parameterisations for atmospheric modelsThe ability to quantify INP spectra (INP concentrations as a function of temperature) and test the efficiency of proxy materials for ice-nucleating efficiency is invaluable for improving our understanding of cloud glaciation and developing representative parameterisations for atmospheric models."

**Formatted:** Font color: Auto

**Deleted:** and the sites on surfaces which cause nucleation at warm temperatures ( $< \sim 10^\circ\text{C}$ ) are rare ( $< 0.1 \text{ L}^{-1}$ )."}

**Deleted:** {DeMott, 2010 #3842}

**Deleted:** However it is not a trivial task, in part because INP concentrations are low and the sites on surfaces which cause nucleation at warm temperatures ( $< \sim 10^\circ\text{C}$ ) are rare

**Deleted:** {Salam, 2006 #1872;Rogers, 2001 #524;Kanji, 2009 #4440;Stetzer, 2008 #4356}{Garimella, 2016 #4357}{Friedman, 2011 #4020}{Glen and Brooks, 2014; Kohn et al., 2016; Kulkarni et al., 2016}

**Deleted:** {Knopf, 2013 #3982;Vali, 2008 #3983;Murray, 2011 #3752;Budke, 2015 #4116;Whale, 2015 #4131;Beall, 2017 #4407;Häusler, 2018 #4444}

**Deleted:** which was

88 *et al.* (2015) and (DeMott et al., 2018). Häusler *et al.* (2018) also presents a summary of the features of various  
 89 techniques. (DeMott et al., 2018)(DeMott et al., 2018)(DeMott et al., 2018)(DeMott et al., 2018),  
 90 A significant challenge in sampling INPs in the atmosphere is their low concentration. At present there is a dearth  
 91 of published, atmospherically relevant, INP measurements globally (Kanji et al., 2017; Vergara-Temprado et al.,  
 92 2017). Not only is the global spatial and temporal coverage of INPs inadequate, but the range of activation  
 93 temperatures and INP concentrations covered in any one set of measurements is typically limited. No single  
 94 instrument has the capability of measuring INP concentrations over the full range of conditions relevant to mixed-  
 95 phase clouds. Online instruments, such as CFDCs, do precisely this, but their detection limit is limited to  $\sim 10^{-1}$   
 96  $L^{-1}$  (Al-Naimi and R., 1985; DeMott et al., 2010; Eidhammer et al., 2010; Prenni et al., 2009). This can be  
 97 improved with aerosol concentrators (Prenni et al., 2013; Tobo et al., 2013), but is still above the INP  
 98 concentrations models suggest influence the properties of certain cloud types, such as high latitude cold-sector  
 99 clouds (Vergara-Temprado et al., 2018). The alternative approach is therefore to increase the number of particles  
 100 within each aliquot of water. In principle, increasing the number of particles per droplet, and therefore the surface  
 101 area of nucleator, per droplet will increase the sensitivity of the experiment to rarer INP. This enables  
 102 quantification of lower INP concentrations. To increase the number of aerosol particles per volume of liquid the  
 103 time period over which an atmospheric sample is collected can be extended, but in doing so temporal resolution  
 104 would be lost. A method of increasing the sensitivity of an immersion mode technique is to increase the volume  
 105 of the collected suspension used in each aliquot, while maintaining the concentration of particles per unit volume.  
 106 This increases the number of particles per aliquot of liquid and therefore makes it more likely that rarer INP will  
 107 be detected. The use of larger volume droplet suspensions has been exploited in the past e.g. (Bigg, 1953; Vali,  
 108 1971), and has been the strategy employed in the development of some recent instruments e.g. (Beall et al., 2017;  
 109 Conen et al., 2012; Du et al., 2017; Stopelli et al., 2014). These large volume assays capture the rarer, more active  
 110 INP but often miss the more abundant but less active INP. Hence they should ideally be used alongside a smaller  
 111 droplet instrument to generate complimentary datasets.  
 112 While many instruments use optical cameras to detect freezing events (Beall et al., 2017; Budke and Koop, 2015;  
 113 Häusler et al., 2018; Whale et al., 2015), some researchers have used techniques to detect the release of latent heat  
 114 associated with freezing. For example, differential scanning calorimetry (Marcolli et al. 2007; Pinti et al. 2012)  
 115 and infrared emissions (Zaragotas et al., 2016; Kunert et al. 2018) have been used. Zaragotas *et al.* (2016) use a  
 116 thermal camera to measure the temperature of individual aliquots within a 96 multiwell plate partially submerged  
 117 within an alcohol bath. This study investigated plant samples but suggested that the technique may be adapted for

**Deleted:**  
**Deleted:** (DeMott et al., 2018)(DeMott et al., 2018)(DeMott et al., 2018) (DeMott et al., 2018) .

**Deleted:** ereby allowing  
**Deleted:** of more active INP  
**Deleted:** An alternative method of increasing the sensitivity of an immersion mode technique is to increase the volume of the collected suspension used in each aliquot. This would increase the number of particles present to act as INP. However it should be clarified that diluting a sample cannot be used to increase the sensitivity of the experiment. Diluting a suspension would reduce the number of particles within a droplet and therefore access regimes where there are more abundant, but less active, INP. Evaporation cannot be used to concentrate filter suspensions either as it may alter the ice-nucleating activity of the INP present or volatiles may be lost in the process.

**Deleted:** }.  
**Deleted:** are frequently  
**Deleted:**  
**Deleted:** achieve  
**Deleted:** a

**Deleted:** Thermal emissions to automate the detection of nucleation events has been used more recently with thermal cameras and differential scanning calorimeters being used to monitor the temperature of droplet arrays (Kunert et al., 2018; Marcolli et al., 2007; Zaragotas et al., 2016).

**Deleted:** (  
**Deleted:** e.g. list three or four from different groups)  
**Deleted:** to detect freezing  
**Deleted:** , some authors have used  
**Deleted:** calorimetry  
**Deleted:** ,  
**Deleted:** while others have used

152 atmospheric purposes. Very recently, Kunert *et al.* (2018) presented a similar set up to investigate biological  
153 samples and collected aerosol. Unlike Zaragotas *et al.* (2016), Kunert *et al.* (2018) do not measure individual  
154 droplet temperatures via infrared emissions but instead use multiple thermistors embedded in the sample holders  
155 to infer temperature for the droplet array.

**Deleted:** and showed the potential for such an instrument

**Deleted:** have utilised

156  
157 Here we propose a new technique, the IR Nucleation by Immersed Particle Instrument (IR-NIPI), for the detection  
158 of INPs using large volumes of sample in the immersion mode. This instrument is part of the NIPI suite of  
159 instruments that includes the  $\mu$ L-NIPI. When used together these devices allow measurements to be taken over a  
160 very wide range of INP concentrations. The use of an infrared camera allows temperature measurements to be  
161 made for individual droplets which helps reduce errors from horizontal gradients across the array of droplets and  
162 the effect of heat release on the temperature of neighbouring wells. The unique design, in combination with a  
163 Stirling engine-based chiller, is also compact making it ideal for field-based measurements and the use of  
164 multiwell plates lends itself to future automation.

**Deleted:** It is a similar technique to that employed by Zaragotas *et al.* (2016) but applied to atmospheric applications with a new novel calibration method.

## 165 2 Instrument Design

### 166 2.1 Operating principle

167 Drop assays have been used extensively for ice nucleation experiments e.g. (Budke and Koop, 2015; Conen *et al.*,  
168 2011; Garcia *et al.*, 2012; Knopf and Forrester, 2011; Stopelli *et al.*, 2014; Vali, 1995, 1971; Whale *et al.*, 2015).  
169 This is partly due to their simplicity compared to other techniques but also the ability to scale the amount of  
170 nucleator with droplet size. In brief, aqueous suspensions are prepared and droplets of a well quantified size are  
171 placed onto a substrate or immersed in oil. These droplets tend to be monodispersed but polydispersed experiments  
172 are also possible (Murray *et al.*, 2011; Vali, 1971). The system is then cooled and the fraction of droplets frozen  
173 is recorded. The cooling can be conducted at a constant rate or with a stepped rate to hold the droplets at a specified  
174 temperature for a period of time (i.e. isothermally) to explore the time dependence aspect of ice nucleation  
175 (Herbert *et al.*, 2014; Sear, 2014; Vali, 1994). The droplets are monitored and the freezing temperature of each  
176 droplet is recorded. The fraction of the droplet population frozen throughout the explored temperature range can  
177 then be determined, from which the ice-nucleating active site density or INP concentration can be derived (Vali  
178 *et al.*, 2015).

184 If the surface area of nucleant per droplet is known then it is common to express the nucleating ability of a material  
185 as the density of active sites per unit surface area of nucleator,  $n_s(T)$  (Connolly et al., 2009; DeMott, 1995). This  
186 approach is based on the assumption specific sites on a nucleator's surface are responsible for ice formation.  $n_s$  is  
187 a cumulative term, i.e. as you move to cooler temperatures there are more features which may behave as an active  
188 site as the energy barrier for ice formation decreases.  $n_s(T)$  is calculated via equation (1).

$$189 \quad n_s(T) = \frac{(-\ln(1 - \frac{n(T)}{N}))}{A} \quad (1)$$

190 Where  $n(T)$  is the number of droplets frozen at a given temperature and  $N$  is the total number of droplets.  $A$  is the  
191 surface area of nucleator within each droplet. Nucleation is a time-dependent stochastic process, but in  
192 determining  $n_s(T)$  the time dependence is neglected. This assumption is justified for many materials because the  
193 diversity in activity of active sites leads to a much greater spread in freezing temperatures than the shift in freezing  
194 temperatures associated with changes in cooling rate (Herbert et al., 2014; Vali, 2008).

## 195 2.2 IR-NIPI design

196 In brief an aqueous suspension is prepared and aliquots pipetted into the wells of a 96 multiwell plate which is  
197 then placed on a temperature controlled stage. The cold stage and multiwell plate are enclosed by a Perspex cover  
198 with an infrared camera mounted in its lid (Figure 1). The system is cooled at  $\sim -1 \text{ }^\circ\text{C min}^{-1}$  until all droplets are  
199 frozen (typically in a temperature range of 0 to  $-30 \text{ }^\circ\text{C}$ ). The temperature of the individual aliquots is monitored  
200 using the IR camera which records a temperature map every 20 seconds. The temperature map is then analysed  
201 with a semi-automated process using custom Python code to yield the freezing temperatures of individual wells.

202 The IR-NIPI has been designed around an Asymptote Ltd. VIA Freeze<sup>TM</sup> stirling cryocooler (Figure 1). The VIA  
203 Freeze uses a Stirling engine to provide a convenient means of cooling without refrigerants or circulating liquids  
204 and was primarily designed for use in cryopreservation applications. This chiller can achieve temperatures of -  
205  $90^\circ\text{C}$ , hence it has more than enough cooling capacity for our application, and has sufficiently low power  
206 requirements that allow it to be run from an automotive 12 V inverter. It also features an onboard datalogger and  
207 internal computer with touch screen control. The VIA Freeze has been developed to accommodate multiwell  
208 plates onto its aluminium cooling stage, which are ideal for large volume drop assays as they hold up to 200  $\mu\text{L}$   
209 per aliquot (for the 96 well plates), allow the separation of droplets to reduce interference across cells and can be  
210 supplied medically sterile. These multiwell plates have anywhere from 12-1536 (with maximum working volumes  
211 of 6.9 mL to 2  $\mu\text{L}$ , respectively). The most useful for this freezing assay are the 96 x 200  $\mu\text{L}$  or 384 x 50  $\mu\text{L}$

Formatted: Font: 10 pt, Not Bold

Formatted: Font: 10 pt, Not Bold, Not Italic, Check spelling and grammar

Deleted: Figure 1

Formatted: Font: 10 pt, Not Bold

Formatted: Font: 10 pt, Not Bold, Not Italic, Check spelling and grammar

Deleted: Figure 1

214 aliquot arrays and in the tests reported here 50  $\mu\text{L}$  droplets (~2300  $\mu\text{m}$  volume equivalent diameter) are used in  
215 96 well plates. We have used both polystyrene (Corning, CLS3788) and polypropylene plates (Greiner, M8060)  
216 and observed no difference in freezing results between the two. To aid thermal contact between the multiwell  
217 plate and the VIA Freeze a thermally conductive gap pad (RS components, 7073452) is located between the cold  
218 plate and the multiwell plate, while a clamping system with screw threads applies mechanical pressure to the  
219 multiwell plate to push the wells into the pad (Figure 1). A specially designed Perspex hood then encloses the  
220 system to reduce contamination from the surroundings. The IR camera slots into the hood and captures an image  
221 of the multiwell plate every 20 seconds (Figure 2a), storing the corresponding temperature data (Figure 2b) on a  
222 removable memory card. The IR camera used here is a Fluke Ti9 Thermal Imager with 160 x 120 pixels. The  
223 Stirling engine chiller is then set to cool down at 1.3  $^{\circ}\text{C min}^{-1}$  which corresponds to 1  $^{\circ}\text{C min}^{-1} \pm 0.06^{\circ}\text{C}$  in the  
224 wells due to a measured offset between the plate and aliquot temperatures. This ramp rate was selected based on  
225 preliminary runs and justification for this cooling rate being equivalent to 1  $^{\circ}\text{C min}^{-1}$  can be seen in the well  
226 temperatures over time (Figure 2b). Once the system has initially cooled to 5  $^{\circ}\text{C}$  the temperature is held for 5 min  
227 to allow time for the system to equilibrate. Following this the system continues to ramp down in temperature while  
228 recording IR heat maps of the multiwell plate.

229 In order to determine the temperature of individual wells, the analysis code locates a pixel centred in the middle  
230 of each well, reporting this temperature as the well temperature. Profiles of temperature versus time are shown in  
231 Figure 2b/c. The freezing temperature of each individual well is determined by comparing each temperature  
232 reading, for a certain well, with the temperature recorded 20 seconds prior. If the temperature reading increases  
233 by more than 2  $^{\circ}\text{C}$  this is recorded as a freezing event (Figure 2c). The 2  $^{\circ}\text{C}$  threshold occasionally needs to be  
234 optimised to capture freezing events while eliminating the detection of false freezing events. For example, samples  
235 that freeze above -3  $^{\circ}\text{C}$  are more difficult to detect because there is less heat released on initial freezing and  
236 crystallisation happens over a longer period of time (see section 2.4). Manual inspection is required in this  
237 temperature regime and the 2  $^{\circ}\text{C}$  threshold adjusted accordingly. The code then prints out the number of events  
238 recorded, along with a time vs temperature plot (Figure 2b) and the corresponding event temperatures for the user  
239 to quality control check and then exports the data as a '.csv' file.

240 The whole process from sample preparation to final analysis takes approximately 1 hour. In order to achieve  
241 higher throughput of samples, albeit with a reduced number of replicates, multiple samples and internal blanks  
242 can be placed within one multiwell plate. For example, when performing dilutions we might run 12 wells as a  
243 handling blank and three lots of 28 wells that contain three different sample dilutions. This not only speeds up

Formatted: Font: 10 pt, Not Bold

Deleted: Figure 1

Formatted: Font: 10 pt, Not Bold, Not Italic, Check spelling and grammar

Formatted: Font: 10 pt, Not Bold

Deleted: Figure 2

Formatted: Font: 10 pt, Not Bold

Deleted: Figure 2

Formatted: Font: 10 pt, Not Bold

Deleted: Figure 2

Formatted: Font: 10 pt, Not Bold

Deleted: Figure 2

Formatted: Font: 10 pt, Not Bold

Deleted: Figure 2

Formatted: Font: 10 pt, Not Bold

Deleted: Figure 2

251 analysis, it also reduces the effect of any time-dependent aging processes such as the rapid deactivation of an  
252 albite sample suspended in water observed by Harrison et al. (2016).

**Deleted:** in an albite sample when suspended in water

**Deleted:** run-to-run variability and the effect of aging of a sample in water which has shown to have implications {Harrison, 2016 #4394}.

### 254 2.3 Temperature measurements with an Infrared camera

255 By using an IR camera to view the thermal emission of each individual well of suspension we are able to obtain  
256 temperatures associated with individual wells. This contrasts with the approaches adopted in other experiments  
257 where the temperature is recorded and assumed to be representative for all droplets, for example when employing  
258 a cold stage housing an embedded thermocouple whose reading is used to represent the temperature of the droplet  
259 array. We note that in our system there was a lateral gradient across the entire multiwell plate in the IR-NIPI of  
260 up to 6 °C (in extreme cases). This is likely due to there not being an even thermal contact of the multiwell plate  
261 with the underlying cold plate. The typical gradient was 4 °C, hence temperature measurements of the individual  
262 wells was necessary.

### 263 2.4 Temperature calibration

264 The IR camera we use was quoted for use between -20 to +250 °C with an uncertainty of ±5 °C and is intended  
265 for use in a wide range of applications with a range of materials of different emissivity. In our application, we  
266 only need to measure the temperature of one material, water, over a relatively narrow range of temperatures, hence  
267 we perform a calibration for our specific experimental setup. Our calibration is based on the fact that when an  
268 aliquot of water in a multiwell plate freezes, the released latent heat raises the temperature of the aliquot to the  
269 ice-water equilibrium temperature (0 °C when the water activity of the sample is ~1, as it is in these experiments).  
270 This is illustrated in Figure 2c which shows the phases of crystallisation that the aliquots go through. Initially, the  
271 crystal growth is rapid with a rapid release of latent heat and a corresponding rise in temperature of the aliquot  
272 within the 20 s time between frames. Visual inspection of the live screen display of the IR camera revealed that  
273 the temperature reached a maximum within 1 s. The temperature of an ice-water mixture will necessarily be 0  
274 °C, hence the aliquot cannot warm above 0 °C and the temperature will remain at 0 °C until all of the water has  
275 frozen and no more heat is evolved. The rate of crystallisation in this regime is determined by the loss of heat to  
276 the surroundings, in this case the cold stage, as well as to the surrounding droplets and the multiwell plate. This  
277 stage of crystallisation takes longer at higher freezing temperatures where the temperature differential between  
278 the cold stage and the aliquot is smaller. Hence, freezing when nucleation takes place at -12 °C takes around 100  
279 s, whereas when nucleation takes place at -20 °C freezing takes around 20-40 s. Once all of the water has frozen

**Commented [AH[2]:** Please note we had email correspondence with G. Vali and decided to add the two sections of text highlighted in red to further explain points that he raised.

**Formatted:** Font: 10 pt, Not Bold

**Deleted:** Figure 2



285 the temperature of the aliquot decreases rapidly back to that of the multiwell plate within 20-40 s. The fact that  
286 the aliquots spend 10s of seconds at 0 °C provides a very useful calibration point for each individual well. In the  
287 following we describe a novel method for calibrating the IR temperature measurements that takes advantage of  
288 this process and proceed to justify this approach.

289 ~~Using the analysis code, an event is identified and recorded. The code then reads the temperature of the frame~~  
290 ~~directly after this freezing event and calculates the difference of this value compared to 0 °C to give an offset~~  
291 ~~correction value, i.e. if the frame after freezing read 2 °C then the correction factor for this well would be -2 °C.~~  
292 ~~This offset value is then subtracted from all of the temperature recordings for that specific well. The average~~  
293 ~~correction value calculated for the IR camera via this method is -1.9 °C with a standard deviation ±0.5 °C.~~ It  
294 should be noted that one of the limitations of the setup used by Zaragotas *et al.* (2016) was that the IR camera was  
295 calibrated only once by the factory, however our calibration method mitigates this limitation.

296 A standard freezing experiment was then performed and the thermocouple data was contrasted to that of the IR  
297 camera which was calibrated using the above method (Figure 3). The comparison in Fig. 3a shows that the IR and  
298 thermocouple temperature were in excellent agreement and this is also readily seen in residuals plotted in Fig 3b.

299 The scatter around the zero line in the residual plot is ± 0.9 °C (two standard deviations) in the regime after the  
300 first equilibrium step at +5 °C and before the first freezing event. We used this value as an estimate of the  
301 temperature uncertainty associated with the IR technique generally. ~~We did not use data in the red and blue shaded~~  
302 ~~areas of Fig. 3b to calculate this uncertainty. The temperature readings in the red shaded area were discarded as~~  
303 ~~they had not been held at +5 °C for five minutes to equilibrate. Temperature readings after the initial freezing~~  
304 ~~event were also discarded as thermal conductivity of ice is different to that of water and neighbouring wells release~~  
305 ~~heat on freezing which influence the temperature of surrounding wells.~~

306 We also tested the IR temperature measurement using T type thermocouples distributed in specific wells of a  
307 polypropylene multiwell plate. The IR camera could not take an accurate reading of wells that had a thermocouple  
308 placed inside them, therefore neighbouring unfrozen wells were assumed to be representative of each other (see  
309 inset in Figure 4). ~~As mentioned above, there is a gradient across the entire plate (Fig. 2A) and so a series of~~  
310 preliminary experiments were undertaken to find suitable placement locations for the thermocouples in which the  
311 surrounding wells displayed similar temperature readings compared to one another. The thermocouples were  
312 placed in the base of the well along with 50 µL of Milli-Q grade water and four surrounding well temperatures

**Deleted:** This offset is likely the result of the initial imprecision of the factory calibration which is designed to cover a wide range of temperatures (-20 °C to +250 °C).

**Formatted:** Font color: Red

**Formatted:** Font color: Red

**Deleted:** this new novel

**Deleted:** could

**Deleted:** We performed a number of experiments to test the IR temperature measurement calibrated using the above method. In the first instance we used highly conductive individual anodised aluminium wells for 50µL droplets. The temperature of three of these wells were recorded independently using T type thermocouples embedded in the aluminium wells to give a representative temperature of the well and aliquot of water (see inset in Figure 3).

**Formatted:** Font: 10 pt, Not Bold

**Formatted:** Font: 10 pt, Not Bold, Not Italic, Check spelling and grammar

**Deleted:**

**Formatted:** Font color: Red

**Formatted:** Font color: Red

**Deleted:** to help minimise the vertical gradients within the well and so the IR camera would likely reading be reading a warmer droplet surface temperature

**Formatted:** Font color: Red

**Formatted:** Font color: Red

**Deleted:** the emissivity and

**Deleted:** . Our IR camera is factory calibrated to use the emissivity of water. There is also the possibility of

**Formatted:** Font color: Red

**Deleted:** ing

**Formatted:** Font color: Red

**Deleted:** could influence the temperature readings, which we cannot quantify the extent of.

**Formatted:** Font color: Red

**Formatted:** Font color: Red

**Formatted:** Font: 10 pt, Not Bold

**Deleted:** Figure 4

**Deleted:**

338 were measured using the IR system. The thermocouple wire crossed one of the four IR measured wells and so  
339 only three wells adjacent to the thermocouple monitored well were used for comparison.

340 A total of six IR measurements were recorded with the corresponding thermocouple readings over a series of  
341 experiments spanning a temperature range of 20 °C to -25 °C. An example of a thermocouple measurement  
342 contrasted to three IR measurements can be seen in [Figure 4a](#). The residual temperatures for all six thermocouple  
343 temperatures are also shown ([Figure 4b](#)). The IR temperature uncertainty derived from the aluminium well  
344 experiment is also plotted and shows that the data is consistent across both strategies with an uncertainty of  $\pm 0.9$   
345 °C.

346

### 347 3 Test experiments and analysis

#### 348 3.1 Control experiments

349 In larger volume freezing assays (10s of microliters) it is extremely challenging to remove all background INPs  
350 from the water and substrates, hence freezing is typically observed at temperatures well above what one would  
351 expect for homogenous freezing (Koop and Murray, 2016). Homogeneous nucleation is expected to result in 50  
352 % of 50  $\mu\text{L}$  droplets freezing at around -35 °C, whereas 50 % of the Milli-Q water droplets froze around -22 °C  
353 in our control experiments ([Figure 5](#)). Filtering of the Milli-Q water to 0.2  $\mu\text{m}$  reduced the temperature at which  
354 pure water droplets froze by 2-3 °C. [Sartorius Ministart, non-pyrogenic, single use filters were used for this](#)  
355 [\(product code 17597-K\)](#). Blanks were run initially with entire 96 well plates and then 12 wells of each experiment  
356 thereafter were allocated for an internal blank when testing samples of INPs (i.e. 12 aliquots of Milli-Q water and  
357 84 aliquots of sample suspension). Comparison of fraction frozen curves for typical IR-NIPI blanks with curves  
358 obtained for droplets containing various ice-nucleating materials (discussed below) show that there is a clear  
359 heterogeneous freezing signal ([Figure 5](#)). We hope to improve the baseline in the future (Polen et al., 2018) but  
360 for the purpose of these experiments the nucleants tested were active at sufficiently warm temperatures to be well  
361 above the baseline.

#### 362 3.3 Feldspar chips

363 To further test the temperature readings from the IR-NIPI instrument a set of experiments was performed where  
364 each droplet contained a single ~100  $\mu\text{m}$  sized grain of K-feldspar in both the IR-NIPI and contrasted to the  
365 standard  $\mu\text{L}$ -NIPI employing 1  $\mu\text{l}$  droplets. The  $\mu\text{l}$ -NIPI is a well-established technique (Whale et al., 2015) which

Deleted: Figure 4

Formatted: Font: 10 pt, Not Bold

Deleted: Figure 4

Formatted: Font: 10 pt, Not Bold

Deleted: 1

Deleted: Figure 5

Deleted: 2

Formatted: Font: 10 pt, Not Bold

Formatted: Font: 10 pt, Not Bold, Not Italic, Check spelling and grammar

Formatted: Not Superscript/ Subscript



Formatted: Font: 10 pt, Not Bold

Formatted: Font: 10 pt, Not Bold, Not Italic, Check spelling and grammar

Deleted: Figure 5

Formatted: Line spacing: Double

Deleted: 1

373 compares well with other similar instruments (Hiranuma et al., 2015). ~~The purpose of this experiment was to have~~  
 374 ~~the same amount of material per droplet in each experiment and to have the material at the base of the droplet so~~  
 375 ~~order that the results from the two instruments could be directly compared. In doing so we could investigate the~~  
 376 ~~extent to which the gradient within the 50 µL wells might be a problem.~~ This experiment was adapted from the  
 377 procedure described by Whale *et al.* (2018) and involved taking K-feldspar rich chips from a bulk rock of  
 378 pegmatite and selecting individual grains (pegmatite is an igneous intrusive rock rich in K-feldspar with large  
 379 grain sizes often being larger than 2.5 cm and hence easy to separate). This material was chosen because K-  
 380 feldspar is known to exhibit excellent ice-nucleating properties (Atkinson et al., 2013; Harrison et al., 2016). A  
 381 total of 19 grains were ~100 µm in diameter were separated by eye, assigned a number and their position tracked  
 382 through the course of each experiment. The same feldspar chips were tested in both the µL-NIPI and the IR-NIPI.  
 383 For the IR-NIPI experiments single grains of feldspar were placed into the bottom of a multiwell plate and 50 µL  
 384 of Milli-Q water was then pipetted into each well. The experiment was then carried out as normal and the freezing  
 385 temperatures of the wells were recorded. The grains were then used in the µL-NIPI experiment by placing the  
 386 grains onto a glass cover slip atop a cold plate and pipetting a single 1 µL droplet onto each grain, before carrying  
 387 out a standard µL-NIPI experiment. Briefly, the temperature of the cold plate was reduced at 1 °C min<sup>-1</sup> and the  
 388 temperature of the droplet freezing events recorded via a camera. The resulting fraction frozen plot for this  
 389 experiment can be seen in .  
 390  and the corresponding correlation plot is shown in Figure 6b. The two instruments yielded similar  
 391 fraction frozen curves and the individual feldspar grains nucleated ice at a similar temperature in both experiments.  
 392 The correlation plot in Figure 6b shows that the freezing temperatures of a single grain were not identical in the  
 393 two experiments, which is consistent with the stochastic nature of nucleation at active sites that have a  
 394 characteristic freezing temperature (Vali, 2014, 2008). The agreement between the two instruments suggests that  
 395 the temperature measurement and calibration of the IR-NIPI were robust and that there is no major temperature  
 396 gradient within the aliquots in the multiwell plates.

397

### 398 3.4 NX-illite

399 The mineral dust NX-illite was chosen as a test sample as it has been used in an extensive intercomparison study  
 400 (Hiranuma et al. 2015) and contains some common components which are found in atmospheric mineral dusts  
 401 (Broadley et al., 2012). NX-illite was taken from the same batch as that used by the Leeds group in the Hiranuma

- Moved down [2]:** , a mineral known to exhibit excellent ice-nucleating properties {Atkinson, 2013 #3874;Harrison, 2016 #4394}.
- Field Code Changed**
- Deleted:** The purpose of this experiment was to have the same amount of material per droplet in each experiment and to have the material at the base of the droplet
- Deleted:** in
- Deleted:**
- Deleted:** In doing so we could investigate the extent to which the gradient within the 50 µL wells
- Deleted:** was an
- Deleted:** issue
- Moved (insertion) [2]**
- Deleted:** n
- Deleted:** , a mineral known to exhibit excellent ice-nucleating properties {Atkinson, 2013 #3874;Harrison, 2016 #4394}. We could achieve a similar experiment by making up a suspension and allowing particles to settle over time to the base of the aliquot. However this would introduce uncertainties as a result of aggregation so single grains are used to overcome this.
- Deleted:** . P
- Deleted:** felsic
- Deleted:** minerals (including alkali feldspars)
- Deleted:** The feldspar chips were selected after sorting them by eye
- Deleted:** which
- Deleted:** collected
- Deleted:** (~100 µm in size)
- Deleted:** as described by Whale *et al.* (2015)
- Formatted:** Font: 10 pt, Not Bold
- Deleted:** Figure 6
- Deleted:** a
- Deleted:** ,
- Deleted:** with t
- Deleted:** suggesting
- Deleted:** The agreement also further justified the use of the calibration method developed for the IR camera. The observation that the feldspar grains in the two experiments gave rise to similar results suggests that the IR camera is reporting a representative temperature, within the quoted temperature uncertainties.

442 *et al.* (2015) intercomparison and no further processing of the material was carried out. Aqueous suspensions of  
443 the sample were prepared by weighing a known amount of material and suspending it in a corresponding volume  
444 of water to make up a weight percent suspension (i.e. 0.1 g of mineral in 9.9 g of water to yield a 1 wt%  
445 suspension). NX-illite concentrations of 0.01, 0.1 and 1 wt% were prepared in this manner, and in each case a  
446 Teflon-coated magnetic stirrer bar was used to keep the particles suspended whilst the sample was pipetted into  
447 the wells of the multiwell plate. Each concentration of NX-illite was tested using the IR-NIPI and the resultant  
448 fraction frozen curves are shown in Fig. 5.

449 By employing a suspension of known concentration and composed of a material with a known specific surface  
450 area, the surface area of nucleator per droplet can be calculated and used alongside the fraction frozen curves to  
451 determine  $n_s(T)$ , as described in equation (1). The  $n_s(T)$  derived from IR-NIPI with 0.01, 0.1 and 1 wt% NX-illite  
452 are shown in [Figure 7a](#). They are in good agreement with one another with lower wt% suspensions yielding data at lower  
453 temperatures and higher  $n_s(T)$  values, as expected. The few data points from the 0.01wt% NX-illite run 2 which  
454 appear as outliers may indicate that the particles were not evenly distributed throughout the droplets. Further to  
455 this a freeze thaw experiment of 0.1wt% suspension was conducted where the sample was frozen once, thawed  
456 and then frozen again (see [Figure 8](#)). The agreement between the two runs show that the material did not alter on  
457 freezing.

459 The values of  $n_s(T)$  for NX-illite derived from 0.01-1 wt% suspensions are shown in [Figure 7a](#)  
460 together with the literature data for this material in [Figure 7b](#). This material has also been investigated by Beall *et al.* (2017) using an instrument that also uses 50 $\mu$ L  
461 droplets: the Automated Ice Spectrometer (AIS). The results of Beall *et al.* (2017) are therefore directly  
462 comparable to the results from the IR-NIPI. All of the wet suspension techniques have been grouped together in  
463 black in Fig. 7b, apart from the AIS data shown in green and the IR-NIPI data in red. Both the IR-NIPI and AIS  
464 data are in good agreement with one another. It can be seen that the larger volume assays (IR-NIPI and AIS) give  
465 results towards the upper spread of literature data but are still consistent with other results ([Figure 7b](#)). Dry dispersed techniques have also been plotted as unfilled blue squares in Fig. 7b, but none of these  
466 techniques are sensitive in the range of  $n_s(T)$  seen by the large droplet instruments. The new data from the IR-

**Deleted:** The  $n_s(T)$  values derived from the IR-NIPI for 0.01, 0.1 and 1 wt% NX-illite are shown in Figure 7a. The results demonstrated good agreement with each other and exhibited the expected trend of the droplets containing smaller amounts of nucleant surface area freezing at lower temperatures and having higher  $n_s(T)$  values than the droplets with higher amounts of surface area. Further to this, a freeze-thaw experiment of a 0.1 wt% NX-illite suspension was conducted wherein the sample was frozen once, thawed and then frozen again (see Figure 8). The two runs froze at similar temperatures, as expected, showing good reproducibility with the IR-NIPI technique.

**Deleted:** ¶

**Deleted:** ¶

**Deleted:** T

**Formatted:** Font: (Default) Times New Roman, 10 pt

**Formatted:** Font: 10 pt

**Deleted:** Figure 7

**Formatted:** Font: 10 pt, Not Bold

**Deleted:** be a relic of the issue discussed in the last paragraph of this section

**Formatted:** Font: 10 pt, Not Bold

**Deleted:** Figure 8

**Formatted:** Font: 10 pt

**Formatted:** Font: 10 pt, Not Bold

**Deleted:** Figure 7

**Formatted:** Font: 10 pt

**Formatted:** Font: 10 pt, Not Bold

**Deleted:** Figure 7

**Formatted:** Font: 10 pt

**Formatted:** Font: 10 pt, Not Bold

491 NIPI has extended the dataset for NX-illite to warmer temperatures than in previous measurements, illustrating  
492 the utility of the technique.

493 It should be noted that in preliminary experiments some discrepancies between dilutions of NX-illite were  
494 observed which highlighted the importance of accurately making up suspensions. In the following we note some  
495 issues that had to be solved. In some initial experiments the dilutions of a suspension would yield a higher than  
496 expected  $n_s(T)$ . On further investigation this issue was resolved via gravimetrically weighing suspensions (i.e.  
497 preparing a known mass of a sample in a known mass of water) rather than diluting a bulk stock suspension.  
498 Further to this great care was taken when sampling from the bulk NX-illite sample as to make sure no bias was  
499 introduced when selecting material since a powder can separate on the basis of grain size. This was avoided by  
500 shaking the container horizontally and selecting material from the centre of the bulk sample. Magnetic stirrer bars  
501 were used to keep particles suspended but when it came to collecting the suspension using a pipette the suspension  
502 was taken from the magnetic stirrer plate to stop the vortex within the vial. As the suspension was not stirring for  
503 a short period of time it meant that particles did not have time to fallout of suspension and there was no longer a  
504 vortex created by the stirrer bar which could bias particle distribution when sampling. The above emphasises the  
505 importance of selecting samples in a repeatable way and may explain some of the variability between the literature  
506 data seen in Fig. 7b.

507

### 508 3.4 Atmospheric aerosol sample

509 In order to demonstrate the utility of this approach for atmospheric aerosol samples, a filter sample was collected  
510 in Leeds as part of a field campaign held on the evening of the 5<sup>th</sup> November. A sample of atmospheric aerosol  
511 was collected using a Mesa PQ100 air sampler for 100 min. An inlet head with an upper cut-off of 10 $\mu$ m was  
512 utilised and air was sampled at 16.7 L min<sup>-1</sup> on to a 0.4  $\mu$ m polycarbonate track-etched Whatman filter, with a  
513 total of 1670 L of air sampled. The filter was then placed into 6 mL of Milli-Q water and vortexed for 5 min to  
514 wash the particles from the filter and into suspension.

Deleted: ¶

515 The aqueous sample was then analysed on the IR-NIPI and  $\mu$ L-NIPI (Whale et al., 2015). The concentration of  
516 INPs per litre of air,  $[INP]_T$ , was subsequently calculated using equation (2) (DeMott et al., 2016).

$$517 [INP]_T = -\ln\left(\frac{Nu(T)}{N}\right)\left(\frac{V_w}{V_a V_s}\right) \quad (2)$$

519 Where  $N_u(T)$  is the number of unfrozen droplets at a given temperature,  $N$  is the total number of droplets,  $V_w$  is  
520 the volume of wash water,  $V_a$  is the volume of an aliquot and  $V_s$  is the volume of air sampled.

521 The resulting INP concentrations from the combination of these two instruments spanned four orders of magnitude  
522 and covered a temperature range of 20°C (see [Figure 9](#)). The data from both instruments was in good agreement  
523 and yielded complementary information. This illustrates how the IR-NIPI can be used to extend the measurements  
524 of INP concentrations to higher temperatures and lower INP concentrations. [Since high-resolution regional  
525 modelling of the effect of INP on low/high latitude, cold sector-clouds suggests that 0.1 to 1 INP L<sup>-1</sup> is a critical  
526 concentration and much lower concentrations still impact clouds](#) (Vergara-Temprado et al., 2018), [measurements  
527 with IR-NIPI will be extremely useful, particularly in environments with low INP concentrations.](#)

**Deleted:** Figure 9

**Formatted:** Font: 10 pt, Not Bold

#### 528 4 Summary and conclusions

529 The IR-NIPI technique is a novel approach to measuring freezing events in immersion mode nucleation studies.

530 [We demonstrate that IR thermometry is a sound method for determining the freezing temperature of 50 µL water  
531 droplets in multiwell plates. This method overcomes potential distorting influences such as thermal gradients  
532 across the plate, the effect of freezing wells warming surrounding wells and poor thermal contact to the underlying  
533 cold plate. A freezing event is detected as a sharp rise in freezing temperature to the equilibrium melting point](#)

**Deleted:** within aliquots

**Deleted:** c

534 [and a novel calibration method has been proposed which relies on the return of water droplets to the equilibrium  
535 melting temperature of water, 0°C, after initial freezing. This gives an individual calibration for every run and  
536 every well. When comparing this calibration technique to thermocouple readings the data is consistent to within  
537 ±0.9°C. The use of this calibration method is further supported when looking at experiments using single grains  
538 of feldspar, with the results being consistent with those of the established µL-NIPI instrument that employs 1µL  
539 droplets on a cold stage. Results for the ice nucleating ability of NX-illite with the IR-NIPI, a mineral dust which  
540 has been the subject of an extensive inter-comparison, are consistent with literature measurements. In particular,  
541 the IR-NIPI is in good agreement with another well-characterised large droplet instrument \(AIS\) \(Beall et al.,  
542 2017\). However, it is unclear why both of these large volume instruments produce  \$n\_s\$  results at the high end of the  
543 range of  \$n\_s\$  values reported previously. \[The utility of IR-NIPI for the analysis of atmospheric samples was also  
544 demonstrated by collecting and analysing an aerosol sample from the city of Leeds, England.\]\(#\) The sample was  
545 analysed simultaneously with the µL-NIPI instrument. Results from the two instruments were in good agreement  
546 with one another. The IR-NIPI instrument extended the range of INP concentrations shown by the µL-NIPI by](#)

**Deleted:** 2 degree shift in temperature to detect freezing events is used and

552 two orders of magnitude, covering a regime critical for cloud formation with a modest sampling time of just 100  
553 mins at 16.67 L min<sup>-1</sup>.

554 **5 REFERENCES**

- 555 Al-Naimi, R. and R., S. C. P.: Measurements of natural deposition and condensation-freezing ice  
556 nuclei with a continuous flow chamber, *Atmos. Environ.*, 19, 1871-1882, 1985.
- 557 Atkinson, J. D., Murray, B. J., Woodhouse, M. T., Whale, T. F., Baustian, K. J., Carslaw, K. S., Dobbie,  
558 S., O'Sullivan, D., and Malkin, T. L.: The importance of feldspar for ice nucleation by mineral dust in  
559 mixed-phase clouds, *Nature*, 498, 355-358, 2013.
- 560 Beall, C. M., Stokes, M. D., Hill, T. C., DeMott, P. J., DeWald, J. T., and Prather, K. A.: Automation and  
561 heat transfer characterization of immersion mode spectroscopy for analysis of ice nucleating  
562 particles, *Atmospheric Measurement Techniques*, 10, 2613-2626, 2017.
- 563 Bigg, E. K.: The supercooling of water, *Proc.Phys. Soc.*, 66, 688-694, 1953.
- 564 Broadley, S. L., Murray, B. J., Herbert, R. J., Atkinson, J. D., Dobbie, S., Malkin, T. L., Condliffe, E., and  
565 Neve, L.: Immersion mode heterogeneous ice nucleation by an illite rich powder representative of  
566 atmospheric mineral dust, *Atmos. Chem. Phys.*, 12, 287-307, 2012.
- 567 Budke, C. and Koop, T.: BINARY: an optical freezing array for assessing temperature and time  
568 dependence of heterogeneous ice nucleation, *Atmos. Meas. Tech.*, 8, 689-703, 2015.
- 569 Conen, F., Henne, S., Morris, C. E., and Alewell, C.: Atmospheric ice nucleators active  $\geq -12^{\circ}\text{C}$  can be  
570 quantified on PM10 filters, *Atmospheric Measurement Techniques*, 5, 321-327, 2012.
- 571 Conen, F., Morris, C. E., Leifeld, J., Yakutin, M. V., and Alewell, C.: Biological residues define the ice  
572 nucleation properties of soil dust, *Atmos. Chem. Phys.*, 11, 9643-9648, 2011.
- 573 Connolly, P. J., Möhler, O., Field, P. R., Saathoff, H., Burgess, R., Choularton, T., and Gallagher, M.:  
574 Studies of heterogeneous freezing by three different desert dust samples, *Atmos. Chem. Phys.*, 9,  
575 2805-2824, 2009.
- 576 Cotton, R. J., Benz, S., Field, P. R., Mohler, O., and Schnaiter, M.: Technical note: A numerical test-  
577 bed for detailed ice nucleation studies in the AIDA cloud simulation chamber, *Atmos. Chem. Phys.*, 7,  
578 243-256, 2007.
- 579 DeMott, P. J.: Quantitative Descriptions of Ice Formation Mechanisms of Silver Iodide-Type Aerosols,  
580 *Atmospheric Research*, 38, 63-99, 1995.
- 581 DeMott, P. J., Hill, T. C., McCluskey, C. S., Prather, K. A., Collins, D. B., Sullivan, R. C., Ruppel, M. J.,  
582 Mason, R. H., Irish, V. E., Lee, T., Hwang, C. Y., Rhee, T. S., Snider, J. R., McMeeking, G. R., Dhaniyala,  
583 S., Lewis, E. R., Wentzell, J. J., Abbatt, J., Lee, C., Sultana, C. M., Ault, A. P., Axson, J. L., Diaz Martinez,  
584 M., Venero, I., Santos-Figueroa, G., Stokes, M. D., Deane, G. B., Mayol-Bracero, O. L., Grassian, V. H.,  
585 Bertram, T. H., Bertram, A. K., Moffett, B. F., and Franc, G. D.: Sea spray aerosol as a unique source of  
586 ice nucleating particles, *Proceedings of the National Academy of Sciences of the United States of*  
587 *America*, 113, 5797-5803, 2016.
- 588 DeMott, P. J., Möhler, O., Cziczo, D. J., Hiranuma, N., Petters, M. D., Petters, S. S., Belosi, F.,  
589 Bingemer, H. G., Brooks, S. D., Budke, C., Burkert-Kohn, M., Collier, K. N., Danielczok, A., Eppers, O.,  
590 Felgitsch, L., Garimella, S., Grothe, H., Herenz, P., Hill, T. C. J., Höhler, K., Kanji, Z. A., Kiselev, A., Koop,  
591 T., Kristensen, T. B., Krüger, K., Kulkarni, G., Levin, E. J. T., Murray, B. J., Nicosia, A., amp, apos,  
592 Sullivan, D., Peckaus, A., Polen, M. J., Price, H. C., Reicher, N., Rothenberg, D. A., Rudich, Y.,  
593 Santachiara, G., Schiebel, T., Schrod, J., Seifried, T. M., Stratmann, F., Sullivan, R. C., Suski, K. J.,  
594 Szakáll, M., Taylor, H. P., Ullrich, R., Vergara-Temprado, J., Wagner, R., Whale, T. F., Weber, D., Welti,  
595 A., Wilson, T. W., Wolf, M. J., and Zenker, J.: The Fifth International Workshop on Ice Nucleation  
596 phase 2 (FIN-02): Laboratory intercomparison of ice nucleation measurements, *Atmospheric*  
597 *Measurement Techniques Discussions*, doi: 10.5194/amt-2018-191, 2018. 1-44, 2018.

Moved (insertion) [3]

598 DeMott, P. J., Prenni, A. J., Liu, X., Kreidenweis, S. M., Petters, M. D., Twohy, C. H., Richardson, M. S.,  
599 Eidhammer, T., and Rogers, D. C.: Predicting global atmospheric ice nuclei distributions and their  
600 impacts on climate, *Proceedings of the National Academy of Sciences, USA*, 107, 11217-11222, 2010.

601 Diehl, K. and Mitra, S. K.: A laboratory study of the effects of a kerosene-burner exhaust on ice  
602 nucleation and the evaporation rate of ice crystals, *Atmospheric Environment*, 32, 3145-3151, 1998.

603 Du, R., Du, P., Lu, Z., Ren, W., Liang, Z., Qin, S., Li, Z., Wang, Y., and Fu, P.: Evidence for a missing  
604 source of efficient ice nuclei, *Sci Rep*, 7, 39673, 2017.

605 Eidhammer, T., DeMott, P. J., Prenni, A. J., Petters, M. D., Twohy, C. H., Rogers, D. C., Stith, J.,  
606 Heymsfield, A., Wang, Z., Pratt, K. A., Prather, K. A., Murphy, S. M., Seinfeld, J. H., Subramanian, R.,  
607 and Kreidenweis, S. M.: Ice Initiation by Aerosol Particles: Measured and Predicted Ice Nuclei  
608 Concentrations versus Measured Ice Crystal Concentrations in an Orographic Wave Cloud, *Journal of  
609 the Atmospheric Sciences*, 67, 2417-2436, 2010.

610 Garcia, E., Hill, T. C. J., Prenni, A. J., DeMott, P. J., Franc, G. D., and Kreidenweis, S. M.: Biogenic ice  
611 nuclei in boundary layer air over two U.S. High Plains agricultural regions, *Journal of Geophysical  
612 Research-Atmospheres*, 117, 2012.

613 Garimella, S., Kristensen, T. B., Ignatius, K., Welti, A., Voigtländer, J., Kulkarni, G. R., Sagan, F., Kok, G.  
614 L., Dorsey, J., Nichman, L., Rothenberg, D., Rösch, M., Kirchgäßner, A., Ladkin, R., Wex, H., Wilson, T.  
615 W., Ladino, L. A., Abbatt, J. P. D., Stetzer, O., Lohmann, U., Stratmann, F., and Cziczo, D. J.: The  
616 SPectrometer for Ice Nuclei (SPIN): An instrument to investigate ice nucleation, *Atmos. Meas. Tech.  
617 Discuss.*, 2016, 1-37, 2016.

618 Hande, L. B. and Hoose, C.: Partitioning the primary ice formation modes in large eddy simulations of  
619 mixed-phase clouds, *Atmospheric Chemistry and Physics*, 17, 14105-14118, 2017.

620 Harrison, A. D., Whale, T. F., Carpenter, M. A., Holden, M. A., Neve, L., apos, Sullivan, D., Vergara  
621 Prado, J., and Murray, B. J.: Not all feldspars are equal: a survey of ice nucleating properties  
622 across the feldspar group of minerals, *Atmospheric Chemistry and Physics*, 16, 10927-10940, 2016.

623 Häusler, T., Witek, L., Felgitsch, L., Hitzemberger, R., and Grothe, H.: Freezing on a Chip—A New  
624 Approach to Determine Heterogeneous Ice Nucleation of Micrometer-Sized Water Droplets,  
625 *Atmosphere*, 9, 140, 2018.

626 Herbert, R. J., Murray, B. J., Dobbie, S. J., and Koop, T.: Sensitivity of liquid clouds to homogenous  
627 freezing parameterizations, *Geophysical Research Letters*, 42, 1599-1605, 2015.

628 Herbert, R. J., Murray, B. J., Whale, T. F., Dobbie, S. J., and Atkinson, J. D.: Representing time-  
629 dependent freezing behaviour in immersion mode ice nucleation, *Atmospheric Chemistry and  
630 Physics*, 14, 8501-8520, 2014.

631 Hiranuma, N., Augustin-Bauditz, S., Bingemer, H., Budke, C., Curtius, J., Danielczok, A., Diehl, K.,  
632 Dreischmeier, K., Ebert, M., Frank, F., Hoffmann, N., Kandler, K., Kiselev, A., Koop, T., Leisner, T.,  
633 Möhler, O., Nillius, B., Peckhaus, A., Rose, D., Weinbruch, S., Wex, H., Boose, Y., DeMott, P. J., Hader,  
634 J. D., Hill, T. C. J., Kanji, Z. A., Kulkarni, G., Levin, E. J. T., McCluskey, C. S., Murakami, M., Murray, B. J.,  
635 Niedermeier, D., Petters, M. D., O'Sullivan, D., Saito, A., Schill, G. P., Tajiri, T., Tolbert, M. A., Welti,  
636 A., Whale, T. F., Wright, T. P., and Yamashita, K.: A comprehensive laboratory study on the  
637 immersion freezing behavior of illite NX particles: a comparison of 17 ice nucleation measurement  
638 techniques, *Atmos. Chem. Phys.*, 15, 2489-2518, 2015.

639 Hoose, C., Kristjánsson, J. E., Chen, J.-P., and Hazra, A.: A Classical-Theory-Based Parameterization of  
640 Heterogeneous Ice Nucleation by Mineral Dust, Soot, and Biological Particles in a Global Climate  
641 Model, *Journal of the Atmospheric Sciences*, 67, 2483-2503, 2010.

642 Hoose, C. and Möhler, O.: Heterogeneous ice nucleation on atmospheric aerosols: a review of results  
643 from laboratory experiments, *Atmos. Chem. Phys.*, 12, 9817-9854, 2012.

644 Kanji, Z. A. and Abbatt, J. P. D.: The University of Toronto Continuous Flow Diffusion Chamber (UT-  
645 CFDC): A Simple Design for Ice Nucleation Studies, *Aerosol Science and Technology*, 43, 730-738,  
646 2009.

647 Kanji, Z. A., Ladino, L. A., Wex, H., Boose, Y., Burkert-Kohn, M., Cziczo, D. J., and Krämer, M.:  
648 Overview of Ice Nucleating Particles, *Meteorological Monographs*, 58, 1.1-1.33, 2017.



649 Knopf, D. A. and Alpert, P. A.: A water activity based model of heterogeneous ice nucleation kinetics  
650 for freezing of water and aqueous solution droplets, *Faraday Discuss*, 165, 513-534, 2013.

651 Knopf, D. A. and Forrester, S. M.: Freezing of Water and Aqueous NaCl Droplets Coated by Organic  
652 Monolayers as a Function of Surfactant Properties and Water Activity, *J. Phys. Chem. A*, 115, 5579-  
653 5591, 2011.

654 Kohn, M., Lohmann, U., Welti, A., and Kanji, Z. A.: Immersion mode ice nucleation measurements  
655 with the new Portable Immersion Mode Cooling Chamber (PIMCA), *Journal of Geophysical Research:*  
656 *Atmospheres*, 121, 4713-4733, 2016.

657 Koop, T. and Murray, B. J.: A physically constrained classical description of the homogeneous  
658 nucleation of ice in water, *J Chem Phys*, 145, 211915, 2016.

659 Kunert, A. T., Lamneck, M., Helleis, F., Pöhlker, M. L., Pöschl, U., and Fröhlich-Nowoisky, J.: Twin-  
660 plate ice nucleation assay (TINA) with infrared detection for high-throughput droplet freezing  
661 experiments with biological ice nuclei in laboratory and field samples, *Atmospheric Measurement*  
662 *Techniques Discussions*, doi: 10.5194/amt-2018-230, 2018. 1-25, 2018.

663 Murray, B. J., Broadley, S. L., Wilson, T. W., Atkinson, J. D., and Wills, R. H.: Heterogeneous freezing  
664 of water droplets containing kaolinite particles, *Atmospheric Chemistry and Physics*, 11, 4191-4207,  
665 2011.

666 Murray, B. J., O'Sullivan, D., Atkinson, J. D., and Webb, M. E.: Ice nucleation by particles immersed in  
667 supercooled cloud droplets, *Chemical Society Reviews*, 41, 6519-6554, 2012.

668 Niemand, M., Möhler, O., Vogel, B., Vogel, H., Hoose, C., Connolly, P., Klein, H., Bingemer, H.,  
669 DeMott, P., Skrotzki, J., and Leisner, T.: A Particle-Surface-Area-Based Parameterization of  
670 Immersion Freezing on Desert Dust Particles, *Journal of the Atmospheric Sciences*, 69, 3077-3092,  
671 2012.

672 Pinti, V., Marcolli, C., Zobrist, B., Hoyle, C. R., and Peter, T.: Ice nucleation efficiency of clay minerals  
673 in the immersion mode, *Atmos. Chem. Phys. Discuss.*, 12, 3213-3261, 2012.

674 Pitter, R. L. and Pruppacher, H. R.: Wind-tunnel investigation of freezing of small water drops falling  
675 at terminal velocity in air, *Quarterly Journal of the Royal Meteorological Society*, 99, 540-550, 1973.

676 Polen, M., Brubaker, T., Somers, J., and Sullivan, R. C.: Cleaning up our water: reducing interferences  
677 from non-homogeneous freezing of

678 "pure" water in droplet freezing assays of ice nucleating particles, *Atmospheric Measurement*  
679 *Techniques Discussions*, doi: <https://doi.org/10.5194/amt-2018-134>, 2018. 1-31, 2018.

680 Prenni, A. J., Demott, P. J., Rogers, D. C., Kreidenweis, S. M., McFarquhar, G. M., and Zhang, G.: Ice  
681 nuclei characteristics from M-PACE and their relation to ice formation in clouds, *Tellus*, 61, 436-448,  
682 2009.

683 Prenni, A. J., Tobo, Y., Garcia, E., DeMott, P. J., Huffman, J. A., McCluskey, C. S., Kreidenweis, S. M.,  
684 Prenni, J. E., Pöhlker, C., and Pöschl, U.: The impact of rain on ice nuclei populations at a forested  
685 site in Colorado, *Geophysical Research Letters*, 40, 227-231, 2013.

686 Rogers, D. C., DeMott, P. J., Kreidenweis, S. M., and Chen, Y. L.: A continuous-flow diffusion chamber  
687 for airborne measurements of ice nuclei, *J. Atmos. Ocean. Tech.*, 18, 725-741, 2001.

688 Salam, A., Lohmann, U., Crenna, B., Lesins, G., Klages, P., Rogers, D., Irani, R., MacGillivray, A., and  
689 Coffin, M.: Ice nucleation studies of mineral dust particles with a new continuous flow diffusion  
690 chamber, *Aerosol. Sci. Tech.*, 40, 134-143, 2006.

691 Sear, R. P.: Quantitative studies of crystal nucleation at constant supersaturation: experimental data  
692 and models, *CrystEngComm*, 16, 6506-6522, 2014.

693 Stetzer, O., Baschek, B., Lüönd, F., and Lohmann, U.: The Zurich Ice Nucleation Chamber (ZINC)-A  
694 new instrument to investigate atmospheric ice formation, *Aerosol Science and Technology*, 42, 64-  
695 74, 2008.

696 Stopelli, E., Conen, F., Zimmermann, L., Alewell, C., and Morris, C. E.: Freezing nucleation apparatus  
697 puts new slant on study of biological ice nucleators in precipitation, *Atmospheric Measurement*  
698 *Techniques*, 7, 129-134, 2014.

699 Tobo, Y., Prenni, A. J., DeMott, P. J., Huffman, J. A., McCluskey, C. S., Tian, G., Pöhlker, C., Pöschl, U.,  
700 and Kreidenweis, S. M.: Biological aerosol particles as a key determinant of ice nuclei populations in  
701 a forest ecosystem, *Journal of Geophysical Research: Atmospheres*, 118, 10,100-110,110, 2013.  
702 Vali, G.: Freezing Rate Due to Heterogeneous Nucleation, *Journal of the Atmospheric Sciences*, 51,  
703 1843-1856, 1994.  
704 Vali, G.: Interpretation of freezing nucleation experiments: singular and stochastic; sites and  
705 surfaces, *Atmospheric Chemistry and Physics*, 14, 5271-5294, 2014.  
706 Vali, G.: Principles of Ice Nucleation. In: *Biological Ice Nucleation and Its Applications*, Lee Jr, R.,  
707 Warren, G. J., and Gusta, L. V. (Ed.), American Phytopathological Society, St. Paul, Mn, USA, 1995.  
708 Vali, G.: Quantitative Evaluation of Experimental Results an the Heterogeneous Freezing Nucleation  
709 of Supercooled Liquids, *Journal of the Atmospheric Sciences*, 28, 402-409, 1971.  
710 Vali, G.: Repeatability and randomness in heterogeneous freezing nucleation, *Atmos. Chem. Phys.*, 8,  
711 5017-5031, 2008.  
712 Vali, G., DeMott, P. J., Möhler, O., and Whale, T. F.: Technical Note: A proposal for ice nucleation  
713 terminology, *Atmos. Chem. Phys.*, 15, 10263-10270, 2015.  
714 Vergara-Temprado, J., Miltenberger, A. K., Furtado, K., Grosvenor, D. P., Shipway, B. J., Hill, A. A.,  
715 Wilkinson, J. M., Field, P. R., Murray, B. J., and Carslaw, K. S.: Strong control of Southern Ocean cloud  
716 reflectivity by ice-nucleating particles, *Proceedings of the National Academy of Sciences of the*  
717 *United States of America*, 115, 2687-2692, 2018.  
718 Vergara-Temprado, J., Murray, B. J., Wilson, T. W., amp, apos, Sullivan, D., Browse, J., Pringle, K. J.,  
719 Ardon-Dryer, K., Bertram, A. K., Burrows, S. M., Ceburnis, D., DeMott, P. J., Mason, R. H., amp, apos,  
720 Dowd, C. D., Rinaldi, M., and Carslaw, K. S.: Contribution of feldspar and marine organic aerosols to  
721 global ice nucleating particle concentrations, *Atmos. Chem. Phys.*, 17, 3637-3658, 2017.  
722 Whale, T. F., Holden, M. A., Kulak, A. N., Kim, Y. Y., Meldrum, F. C., Christenson, H. K., and Murray, B.  
723 J.: The role of phase separation and related topography in the exceptional ice-nucleating ability of  
724 alkali feldspars, *Phys Chem Chem Phys*, 19, 31186-31193, 2017.  
725 Whale, T. F., Holden, M. A., Wilson, T. W., O'Sullivan, D., and Murray, B. J.: The enhancement and  
726 suppression of immersion mode heterogeneous ice-nucleation by solutes, *Chem Sci*, 9, 4142-4151,  
727 2018.  
728 Whale, T. F., Murray, B. J., O'Sullivan, D., Wilson, T. W., Umo, N. S., Baustian, K. J., Atkinson, J. D.,  
729 Workneh, D. A., and Morris, G. J.: A technique for quantifying heterogeneous ice nucleation in  
730 microlitre supercooled water droplets, *Atmos. Meas. Tech.*, 8, 2437-2447, 2015.  
731 Zarogotas, D., Liolios, N. T., and Anastassopoulos, E.: Supercooling, ice nucleation and crystal growth:  
732 a systematic study in plant samples, *Cryobiology*, 72, 239-243, 2016.

733

734

735

736

737

738

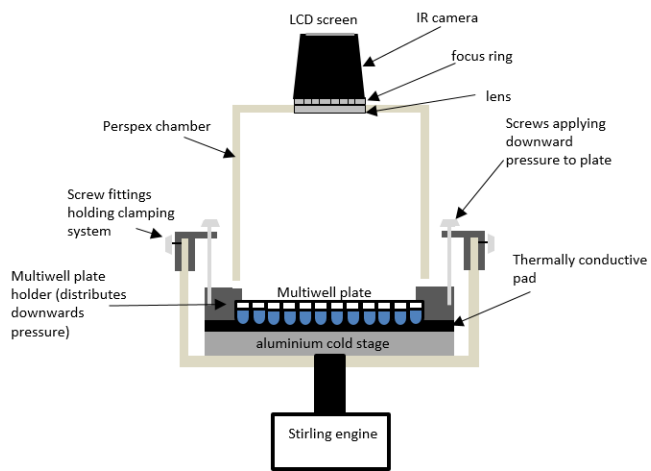
739

740

741

742

743



744

745 **Figure 1.** Schematic diagram of the IR-NIPI system (not to scale). The IR camera is positioned above the multiwell plate and monitors the  
746 freezing events as the cold stage cools.

747

748

749

750  
751  
752  
753  
754  
755  
756  
757  
758  
759  
760  
761  
762  
763  
764  
765  
766  
767  
768  
769  
770  
771  
772  
773  
774  
775  
776  
777

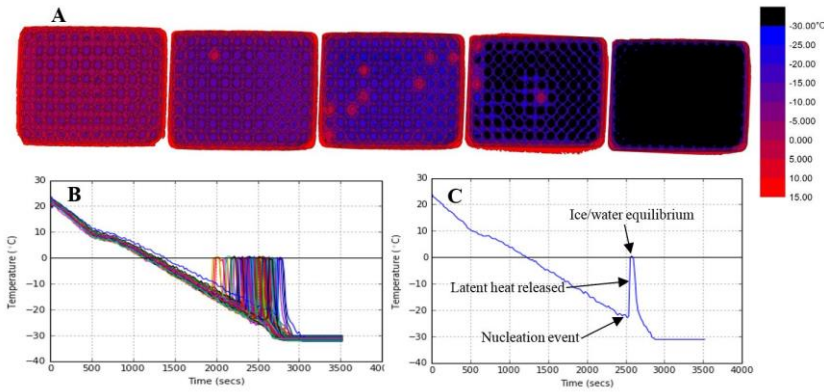


**Figure 2.** (A) Demonstrates a sequence of colour maps taken during the course of an experiment. The leftmost image shows the start of an experiment with all droplets unfrozen, moving to all droplets frozen in the right most image. Warmer temperatures are represented in red, transitioning to blue for colder temperatures and finally black at  $-30^{\circ}\text{C}$  and below. (B) An example of the output of each experiment with the temperature of the 96 wells plotted against time. The spikes in temperature are related to ice formation. The gradient of the decreasing temperature is consistent with that of  $1^{\circ}\text{C min}^{-1}$ . The calibration described in section 2.2 was applied here. Note that one well had a higher temperature than the others, likely due to poor thermal contact with the aluminium substrate. By using IR thermometry to measure the temperature of each well individually such variability is accounted for. (C) Plot of temperature vs time for a single well within a multiwell plate containing  $50\mu\text{L}$ s of water.

Deleted:

Deleted: this is an advantage of using IR thermometry to determine the temperature of each well individually.

781

782

783

784

785

786

787

788

789

790

791

792

793

794

795

796

797

798

799

800

801

802

803

804

805

806

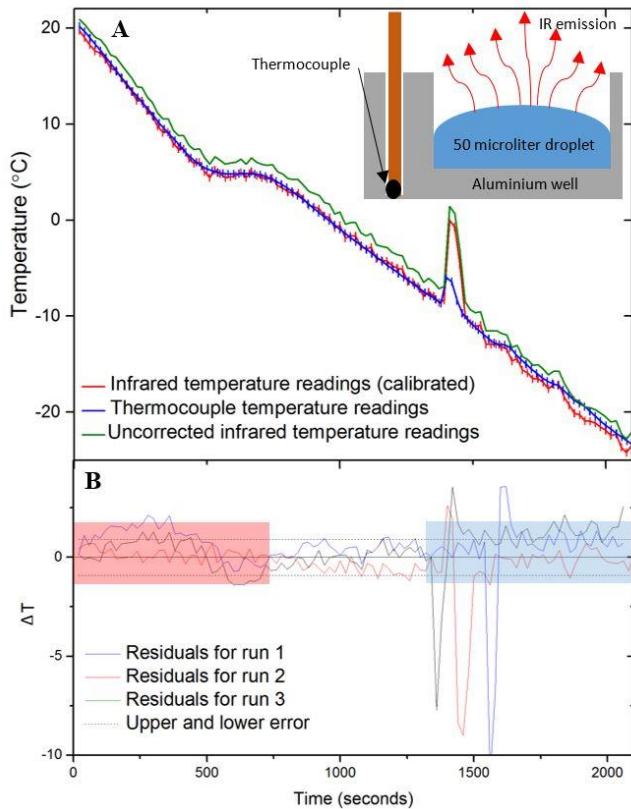
807

808

809

810

811



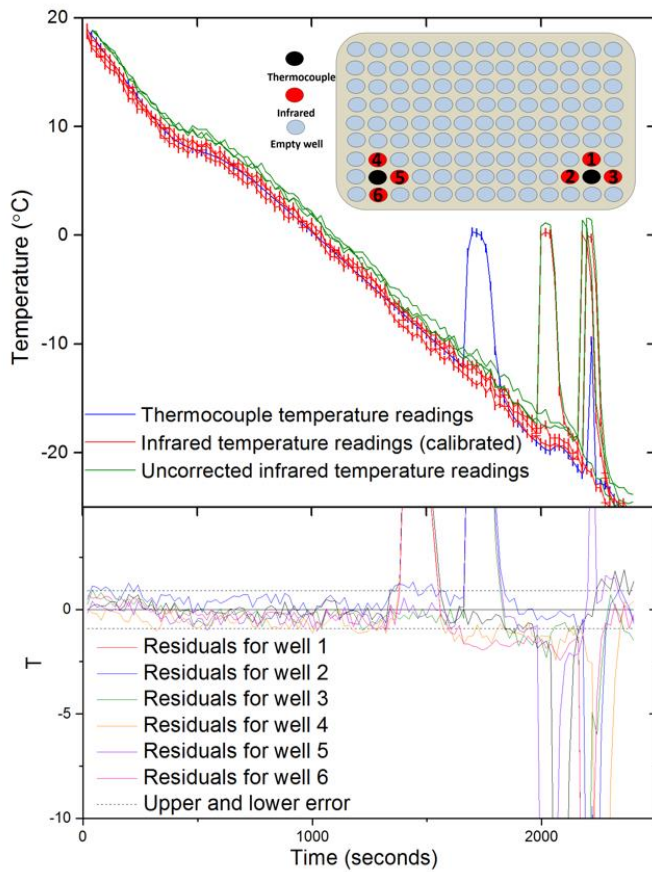
812

**Figure 3.** (A) Plot showing a temperature measurement from a thermocouple (shown in blue) placed within an aluminium well vs infrared measurements taken using the IR camera. Uncorrected IR data is shown in green, whilst corrected IR data following the calibration described in section 2.2 is shown in red. Inset is a schematic of the experimental setup. (B) Plot illustrating the difference in temperature between the thermocouple readings for three aluminium wells and the corresponding IR data. The difference was calculated by  $IR(T) - Thermocouple(T)$ . The negative spikes are a result of the IR camera directly reading the water temperature as it is heated by ice formation whereas the thermocouple measurement is reading the temperature of the aluminium well which is less affected by the latent heat release. The calculated error in temperature for the IR camera of  $\pm 0.9^{\circ}C$  is shown in dashed lines. The range over which freezing occurs is highlighted with a blue rectangle as this is where the thermal properties of ice and the initiation of heat release affect the temperature readings. Highlighted in red is the section of data before the well has equilibrated and so the IR camera is likely reading a warmer surface temperature than the thermocouple.

**Deleted:** , but the temperature of the Al well lags behind

**Deleted:** whereas the thermocouple measurement is reading the temperature of the aluminium well which is less effected by the latent heat release.

**Deleted:** The range of freezing is highlighted in blue as this is where the thermal properties of ice and the initiation of heat release will affect the temperature readings



820

821 **Figure 4.** (A) Plot showing a temperature measurement from a thermocouple placed within a polyethylene well vs three infrared measurements  
 822 of surrounding wells corrected using the calibration described in section 2.2. The uncorrected IR data can be seen in green, with the corrected  
 823 IR data in red and the thermocouple readings in blue. A diagram of the wells within a 96 well plate chosen for the comparison of IR and  
 824 thermocouple measurements is displayed as an inset. The numbers of the wells correspond to the residuals in part B. Red wells represent the  
 825 wells measured with the infrared camera and black wells represent those measured with thermocouples. It should be noted that one of the four  
 826 surrounding IR well temperature readings was discarded from each experiment as the thermocouple wire impeded the temperature  
 827 measurement. Note that the freezing events at ~2000s appear to cause some heating in the adjacent well. (B) Plot of the difference in  
 828 temperature between the thermocouple readings for two wells and six corresponding wells measured with the IR camera. The difference was  
 829 calculated by  $IR(T) - Thermocouple(T)$ . The calculated error in temperature for the IR camera is shown in dashed lines ( $\pm 0.9^{\circ}C$ ). The range  
 830 of freezing is highlighted in blue as this is where the thermal properties of ice and the initiation of heat release will affect the temperature  
 831 readings. Highlighted in red is the section of data before the well had equilibrated and so the IR camera was likely reading a warmer surface  
 832 temperature than the thermocouple.

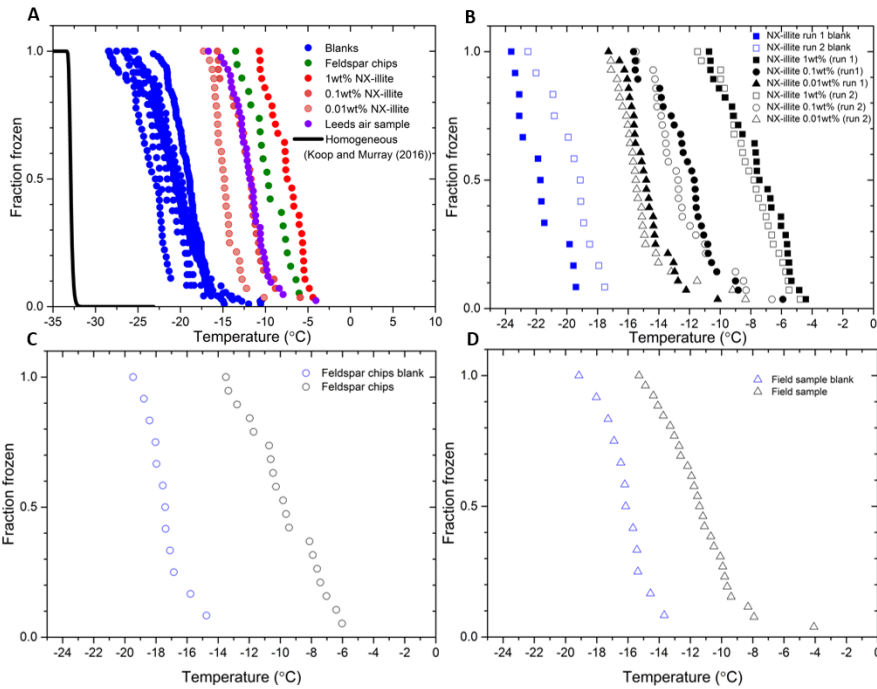
833

834

835

Formatted: Font: (Default) Times New Roman, 12 pt

Deleted: A schematic diagram of the wells within a 96 well plate chosen for the comparison of IR and thermocouple measurements is displayed.



Formatted: Font: (Default) Times New Roman, 12 pt

Formatted: Normal, Line spacing: Double

841 **Figure 5.** (A) Plot of the fraction frozen curves for the IR-NIPI experiment showing standard blank runs and the sample runs from this study.  
 842 Homogeneous freezing of water as predicted with the Koop and Murray (2016) parameterisation is also shown in black. (B) Fraction frozen  
 843 plot for the internal blanks versus the corresponding NX-illite runs. (C) Fraction frozen plot for the internal blank versus the corresponding  
 844 feldspar chips run. (D) Fraction frozen plot for the internal blank versus the corresponding field sample run.

Deleted: ¶  
 <object>¶  
 ¶  
 ¶  
 ¶  
 ¶  
 ¶  
 ¶  
 ¶

Formatted: Font: (Default) Times New Roman, 12 pt

Formatted: Font: (Default) +Body (Calibri), 11 pt, Not Bold, Italic

Deleted: s

Deleted: ns

Formatted: Font color: Text 1

Formatted: Font color: Text 1

Formatted: Font color: Text 1

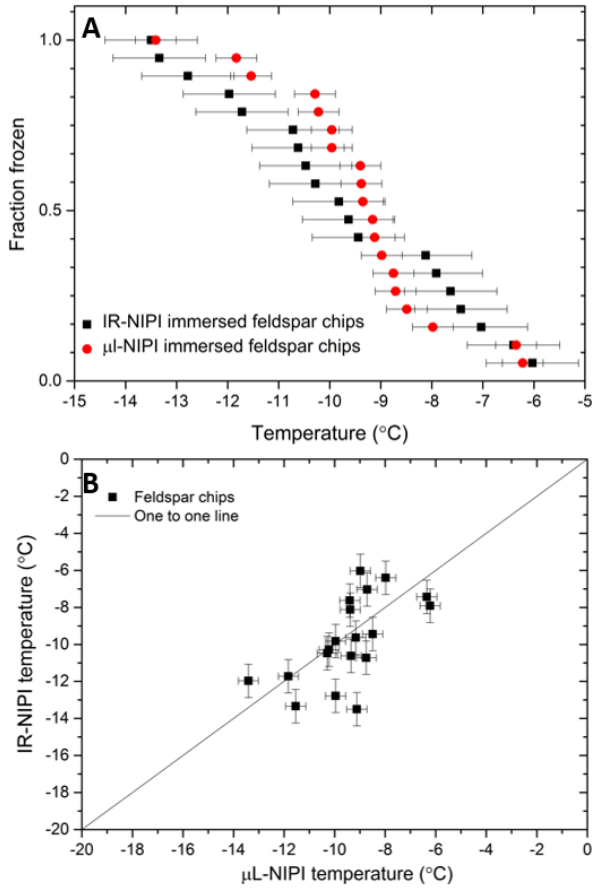
Formatted: Font color: Text 1

Formatted: Font color: Text 1

Formatted: Font color: Text 1

860

Formatted: Font: (Default) Times New Roman, 12 pt



861

862

863

864

865

866

867

**Figure 6. (A)** Plot of the fraction frozen curves for single feldspar particles per droplet in both the  $\mu\text{L-NIPI}$  (using 1  $\mu\text{L}$  droplets) and IR-NIPI (using 50  $\mu\text{L}$  droplets) experiments. The error bars display the error in temperature measurement on both instruments. **(B)** Shows the freezing temperature for the individual feldspar chips as measured by the IR-NIPI and  $\mu\text{L-NIPI}$  instruments. The one to one line is shown in bold and the error in temperature for the two instruments are represented by the error bars.

Deleted: ¶

Formatted: Justified, Line spacing: Double

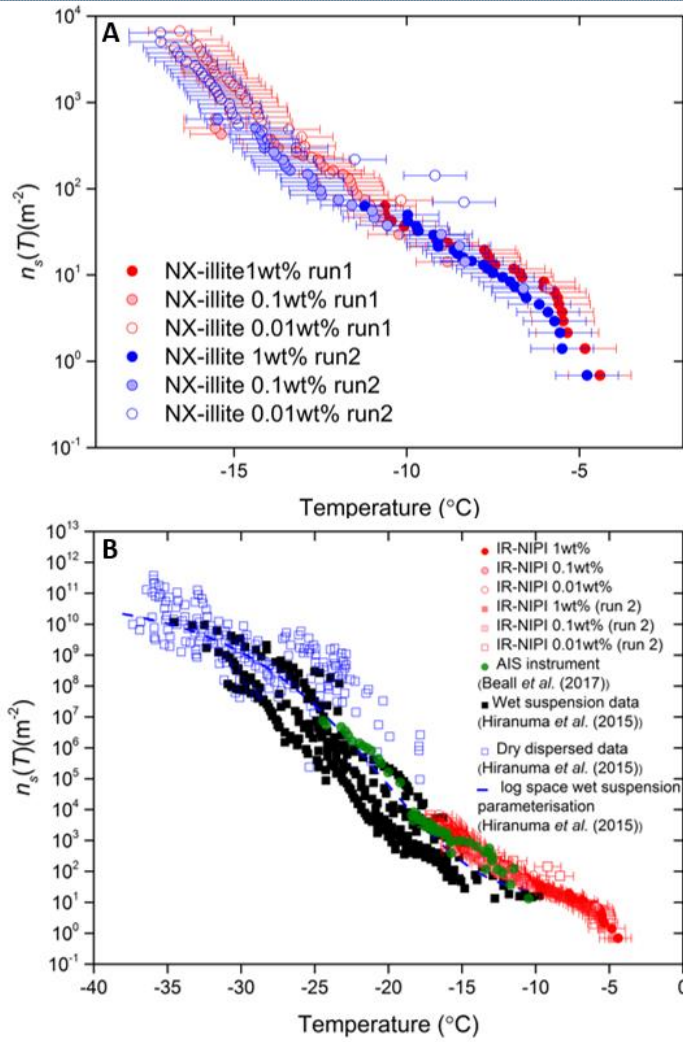
Deleted: ¶

Formatted: Left

Deleted: -----Page Break-----



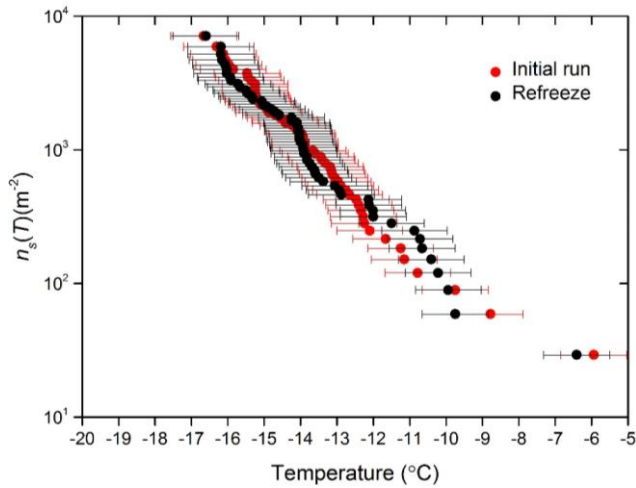
893  
 894  
 895  
 896  
 897  
 898  
 899  
 900  
 901  
 902  
 903  
 904  
 905  
 906  
 907  
 908  
 909  
 910  
 911  
 912  
 913  
 914  
 915  
 916  
 917  
 918



Formatted: Font: (Default) Times New Roman, 8 pt  
 Deleted: <object>  
 Formatted: Font: (Default) Times New Roman, 8 pt

**Figure 7.** (A) The active site density,  $n_s(T)$ , for a dilution series of NX-illite run on the IR-NIPI instrument. The data for a repeat experiment is also shown. The error bars represent the temperature error of  $\pm 0.9^{\circ}\text{C}$ . (B) Plot of the active site density vs temperature for an array of techniques investigating NX-illite. Data from wet dispersed techniques are displayed in black with the IR-NIPI highlighted in red and Automated Ice Spectrometer (AIS) in green. Data from dry dispersed techniques are also plotted as hollow blue squares.

920  
921



922  
923  
924  
925  
926  
927  
928  
929  
930  
931

Figure 8. Plot of the active site density,  $n_s(T)$ , for a 0.01wt% NX-illite suspension and its corresponding refreeze run after the droplets had been thawed out.

932  
933  
934  
935  
936  
937  
938  
939  
940  
941  
942  
943  
944

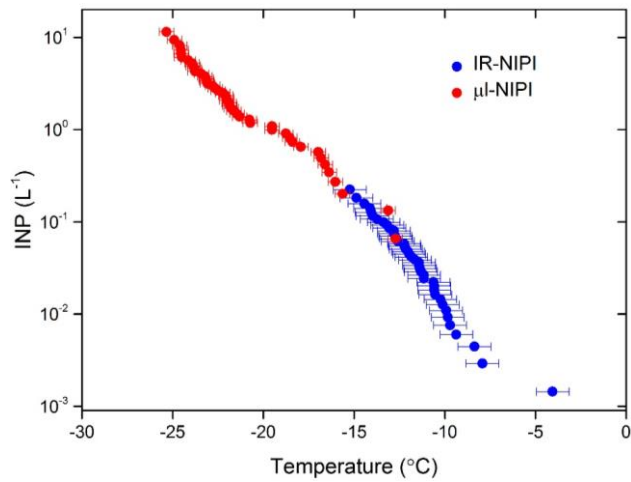


Figure 9. INP concentrations per litre of sampled air during a field campaign. INP concentrations are displayed for the IR-NIPI and  $\mu\text{L-NIPI}$ .

945  
946  
947  
948  
949  
950

Deleted: ¶  
 Formatted: Line spacing: Multiple 1.08 li  
 Formatted: Font: Bold

Deleted: ¶

Deleted: ¶  
¶

**Moved up [3]:** Al-Naimi, R. and R., S. C. P.: Measurements of natural deposition and condensation-freezing ice nuclei with a continuous flow chamber, *Atmos. Environ.*, 19, 1871-1882, 1985.¶

Atkinson, J. D., Murray, B. J., Woodhouse, M. T., Whale, T. F., Baustian, K. J., Carslaw, K. S., Dobbie, S., O'Sullivan, D., and Malkin, T. L.: The importance of feldspar for ice nucleation by mineral dust in mixed-phase clouds, *Nature*, 498, 355-358, 2013.¶

Beall, C. M., Stokes, M. D., Hill, T. C., DeMott, P. J., DeWald, J. T., and Prather, K. A.: Automation and heat transfer characterization of immersion mode spectroscopy for analysis of ice nucleating particles, *Atmospheric Measurement Techniques*, 10, 2613-2626, 2017.¶

Bigg, E. K.: The supercooling of water, *Proc.Phys. Soc.*, 66, 688-694, 1953.¶

Broadley, S. L., Murray, B. J., Herbert, R. J., Atkinson, J. D., Dobbie, S., Malkin, T. L., Condliffe, E., and Neve, L.: Immersion mode heterogeneous ice nucleation by an illite rich powder representative of atmospheric mineral dust, *Atmos. Chem. Phys.*, 12, 287-307, 2012.¶

Budke, C. and Koop, T.: BINARY: an optical freezing array for assessing temperature and time dependence of heterogeneous ice nucleation, *Atmos. Meas. Tech.*, 8, 689-703, 2015.¶

Conen, F., Henne, S., Morris, C. E., and Alewell, C.: Atmospheric ice nucleators active  $\geq -12^\circ\text{C}$  can be quantified on PM10 filters, *Atmospheric Measurement Techniques*, 5, 321-327, 2012.¶

Conen, F., Morris, C. E., Leifeld, J., Yakutin, M. V., and Alewell, C.: Biological residues define the ice nucleation properties of soil dust, *Atmos. Chem. Phys.*, 11, 9643-9648, 2011.¶

Connolly, P. J., Möhler, O., Field, P. R., Saathoff, H., Burgess, R., Choulaton, T., and Gallagher, M.: Studies of heterogeneous freezing by three different desert dust samples, *Atmos. Chem. Phys.*, 9, 2805-2824, 2009.¶

Cotton, R. J., Benz, S., Field, P. R., Mohler, O., and Schnaiter, M.: Technical note: A numerical test-bed for detailed ice nucleation studies in the AIDA cloud simulation chamber, *Atmos. Chem. Phys.*, 7, 243-256, 2007.¶

DeMott, P. J.: Quantitative Descriptions of Ice Formation Mechanisms of Silver Iodide-Type Aerosols, *Atmospheric Research*, 38, 63-99, 1995.¶

DeMott, P. J., Hill, T. C., McCluskey, C. S., Prather, K. A., Collins, D. B., Sullivan, R. C., Ruppel, M. J., Mason, R. H., Irish, V. E., Lee, T., Hwang, C. Y., Rhee, T. S., Snider, J. R., McMeeking, G. R., Dhaniyala, S., Lewis, E. R., Wentzell, J. J., Abbatt, J., Lee, C., Sultana, C. M., Ault, A. P., Axson, J. L., Diaz Martinez, M., Venero, I., Santos-Figueroa, G., Stokes, M. D., Deane, G. B., Mayol-Bracero, O. L., Grassian, V. H., Bertram, T. H., Bertram, A. K., Moffett, B. F., and Franc, G. D.: Sea spray aerosol as a unique source of ice nucleating particles,